Quantitative fingerprinting by headspace—Two-dimensional comprehensive gas chromatography–mass spectrometry of solid matrices: Some challenging aspects of the exhaustive assessment of food volatiles

Quantitative fingerprinting by headspace - two-dimensional comprehensive gas chromatography - mass spectrometry of solid matrices: some challenging aspects of the exhaustive assessment of food volatiles

Luca Nicolotti[1], Chiara Cordero[1]*, Cecilia Cagliero[1], Erica Liberto[1], Barbara Sgorbini[1], Patrizia Rubiolo[1] and Carlo Bicchi[1]

[1]Dipartimento di Scienza e Tecnologia del Farmaco, Università di Torino, Via P. Giuria 9, I-10125 Torino, Italy

* Address for correspondence:
Dr. Chiara Cordero - Dipartimento di Scienza e Tecnologia del Farmaco, Università di Torino, Via P. Giuria 9, I-10125 Torino, Italy – e-mail: chiara.cordero@unito.it ; phone: +39 011 6707662; fax: +39 011 2367662

Abstract

The study proposes an investigation strategy that simultaneously provides detailed profiling and quantitative fingerprinting of food volatiles, through a “comprehensive” analytical platform that includes sample preparation by Head Space Solid Phase Microextraction (HS-SPME), separation by two-dimensional comprehensive gas chromatography coupled with mass spectrometry detection (GC×GC-MS) and data processing using advanced fingerprinting approaches.

Experiments were carried out on roasted hazelnuts and on *Gianduja* pastes (sugar, vegetable oil, hazelnuts, cocoa, nonfat dried milk, vanilla flavorings) and demonstrated that the information potential of each analysis can better be exploited if suitable quantitation methods are applied. Quantitation approaches through Multiple Headspace Extraction and Standard Addition were compared in terms of performance parameters (linearity, precision, accuracy, Limit of Detection and Limit of Quantitation) under headspace linearity conditions. The results on 19 key analytes, potent odorants, and technological markers, and more than 300 fingerprint components, were used for further processing to obtain information concerning the effect of the matrix on volatile release, and to produce an informative chemical blueprint for use in sensomics and flavoromics. The importance of quantitation approaches in headspace analysis of solid matrices of complex composition, and the advantages of MHE, are also critically discussed.

KEY-WORDS

two-dimensional comprehensive gas chromatography-mass spectrometry , multiple headspace extraction, quantitative fingerprinting, sensomics, *Corylus avellana* L., detailed profiling

1. INTRODUCTION

The detailed profiling of volatiles from food is informative, not only to assess botanical and geographical origins, but also to classify and qualify samples on the basis of sensory profile (aroma and taste), technological impact or, more in general, quality attributes [1-4].

However, the volatile fraction of foods of plant origin is often a complex mixture of chemicals already present in the raw matrix, and compounds whose formation is mainly due to a number of reactions, primarily those promoted by thermal treatments (i.e., Maillard reaction, Strecker's degradation of amines, thermal degradation of carbohydrates) and/or enzymatic catalysis (i.e., oxidation, hydrolysis, fermentation, etc.). In addition, common pathways underlying the formation of these compounds lead to components having similar physicochemical properties (volatility and polarity); this is challenging for one-dimensional gas chromatographic separation (1D-GC), not least because some components present poorly-diagnostic MS fragmentation patterns, limiting the effectiveness of EI-MS in providing univocal component identification.

In this context, headspace sampling on-line combined with two-dimensional GC-MS can be a successful platform to overcome these limits thanks to the orthogonality of the involved techniques. In particular, headspace-solid phase microextraction (HS-SPME) and two-dimensional gas chromatographic separation (GC×GC) enable to sample and separate volatiles (including aroma active compounds) on the basis of their physicochemical properties (volatility, polarity, partition coefficient, solubility, etc.) while mass spectroscopy (MS) enables reliable identification (exact mass assignment, fragmentation pattern, multiple reaction monitoring), as well as quantitation (true concentration and/or relative abundance). Such a strategy can provide for reliable and detailed profiling (untargeted and targeted) and fingerprinting of the volatile fraction from food [5]. However, to the best of the authors' knowledge, little has been done to develop comprehensive approaches to exploit the full information potential of multidimensional techniques, in terms of both qualitative distribution of volatiles, and quantitative determination of key compounds related to food sensory properties or technological treatments. In the light of this deficiency, the present paper reports and critically discusses the possibility of carrying out detailed profiling and quantitative fingerprinting simultaneously, through the well-known investigation approaches typical of the

67 “omics” disciplines, on a complex thermally-processed solid food matrix of vegetable origin [6-10], i.e.,
68 roasted hazelnuts from different botanical and geographical origins, and a food end-product, *Gianduja*
69 paste, consisting of hazelnuts, cocoa and other ingredients (sugar, nonfat dry milk, and fats of vegetable
70 origin). An analytical strategy is proposed for profiling the volatile fraction sampled by headspace solid
71 phase microextraction (HS-SPME) and quantifying selected target analytes of the investigated matrices,
72 whose aroma profiles are characterized by a peculiar distribution of key odorants (aroma blueprint),
73 In particular, the effectiveness of two quantitation approaches (Standard Addition–SA, and Multiple
74 Headspace Extraction-MHE) was evaluated by validating method performance parameters (accuracy,
75 precision, limit of quantitation-LOQ and limit of detection-LOD) and examining the informative potential of
76 GC×GC-MS results; information was also derived on odorant release from the sample. The performance of
77 the two approaches was examined in terms of providing a detailed profile of targeted and untargeted
78 features of the complete pattern of the volatiles analyzed, through the number of reliably matched
79 features and the target analytes undetectable when headspace linearity conditions are adopted.
80
81 **2. MATERIALS AND METHODS**
82 **2.1 Reference compounds and solvents**
83 Pure reference compounds for quantitative determinations were purchased from Sigma-Aldrich (Milan,
84 Italy); these are listed in **Table 1,** together with their CAS Registry Number, purity, Target Ion (*Ti*) and
85 Qualifiers (*Q1* and *Q2*) adopted for quantitation. The homologue series of *n*-alkanes (from *n*-C9 to *n*-C25)
86 for Linear Retention Index ($\boldsymbol{I^T_S}$) determination were also from Sigma-Aldrich (Milan, Italy). Solvents were all
87 HPLC-grade, from Riedel-de Haen (Seelze, Germany).
88
89 **2.2 Reference solutions and calibration mixtures**
90 Standard stock solutions at 1 µg/mL, containing pure reference compounds, were prepared in dibutyl
91 phtalate (DBP) and stored in a sealed vial at -18°C. Standard spiking solutions, to be adopted for standard
92 addition and external standard calibration, were prepared by diluting standard stock solutions in DBP at
93 final concentrations of 10, 20, 40, 60, 80 and 100 ng/mL for all analytes, with some exceptions, where

94 further dilutions (150, 200 and 250 ng/mL) were included to cover the real-world samples concentration
95 interval (cf. **Table 1**) and in order to avoid any headspace formation. Standard spiking solutions were stored
96 at -18°C.
97 For MHE external calibration, a series of calibrating solutions in cyclohexane was also prepared to obtain
98 full evaporation of reference compounds [11] in order to estimate the contribution made by the analyte
99 partition coefficient (*K*) between solvent (i.e. DBP) or matrix, and headspace in the sampling conditions.
100

101 **2.3 Hazelnut samples and Gianduja paste**

102 Raw hazelnuts (*Corylus avellana* L.) from the 2011 harvest, with a selected caliber of 12-13 mm, were kindly
103 supplied by Ferrero S.p.A. (Alba-CN, Italy). Samples included the mono-cultivar named *Tonda Gentile*
104 *Trilobata* (*TGT*), also known as Nocciola del Piemonte (EU Quality registration code IT/PGI/0217/0305), and
105 a Turkish blend harvested in the Ordu region made up different cultivars: *Tombul, Palaz and Kalinkara*.
106 Samples were roasted in a lab scale ventilated oven, using standardized protocols [4] for mild (170°C for 20
107 minutes – *170-20*) and medium roasting (170°C for 35 minutes – *170-35*) compatible respectively with the
108 preparation of confectionary and ice-cream topping, or of hazelnut paste. Roasting was conducted in two
109 replicate batches (batch #1 and #2) and samples immediately analyzed to avoid any possible variation due
110 to the release of highly volatile compounds or to shelf-life degradation. Hazelnuts were frozen before
111 milling, using liquid nitrogen, to ensure homogeneous particle size distribution.
112 *Gianduja* paste samples (ingredients: sugar, vegetable oil, hazelnuts, cocoa, nonfat milk, vanilla flavorings)
113 were from two manufactures; Samples#1 to #4 were different formulations of the same product, while
114 Sample#5 was a commercial product purchased in a local supermarket.
115

116 **2.4 Headspace Solid Phase Microextraction (HS-SPME) devices and sampling conditions**

117 SPME sampling devices and fibers were from Supelco (Bellefonte, PA, USA). A
118 Divinylbenzene/Carboxen/Polydimethylsiloxane d_f 50/30 µm, 2 cm long fiber was chosen, and conditioned
119 before use as recommended by the manufacturer.

120 Sample preparation varied depending on the approach adopted for quantification (SA or MHE) and was
121 applied to different amounts of ground material, up to the appropriate amount for correct quantification
122 (from 1.500 g to 0.100 g) that is 0.100 g, to achieve headspace linearity for target analytes.
123 In particular, for SA quantification, aliquots of 0.100 grams of ground hazelnuts were sealed in a 20 mL
124 headspace vial and spiked with suitable volumes of standard spiking solutions for each calibration level (cf.
125 **Table 1**). Before extraction, the vial was vortexed for 60 seconds in a Whirlimixer (Fisons- CE Instruments
126 Rodano – Milan Italy) to homogenize the sample. The fiber was then exposed to the headspace for 20
127 minutes at 50°C before analysis.
128 For MHE quantification carried out with the External Standard approach, aliquots of 0.100 grams of ground
129 hazelnuts were sealed in a 20 mL headspace vial and submitted to multiple consecutive extractions (up to
130 four times) exposing the fiber to the headspace for 20 minutes at 50°C before analysis. MHE external
131 calibration was run on suitable volumes of standard spiking solutions at different concentration levels (cf.
132 **Table 1**) and submitting the resulting sample to multiple consecutive extractions (up to four times) before
133 sampling (20 minutes at 50°C) and analysis.
134
135 **2.5 GC×GC-MS instrument set-up**
136 GC×GC analyses were run on an Agilent 6890 GC unit coupled with an Agilent 5975C MS detector operating
137 in EI mode at 70 eV (Agilent, Little Falls, DE, USA). The transfer line was set to 260°C. A *Standard Tune* was
138 used and the scan range was set to m/z 35-240 with a scanning rate of 10,000 amu/s, to obtain an
139 appropriate number of data points for the reliable identification and quantitation of each chromatographic
140 peak. The system was provided with a two-stage KT 2004 loop thermal modulator (Zoex Corporation,
141 Houston, TX) cooled with liquid nitrogen; the hot jet pulse time was set at 250 ms with a modulation time
142 of 4 s, adopted for all experiments. Fused silica capillary loop dimensions were 1.0 m length and 100 µm
143 inner diameter. The column set was configured as follows: ^{1}D SolGel-Wax column (100% polyethylene
144 glycol) (30 m × 0.25 mm d_c, 0.25 µm d_f) coupled with a ^{2}D OV1701 column (86% polydimethylsiloxane, 7%
145 phenyl, 7% cyanopropyl) (1 m × 0.1 mm d_c, 0.10 µm d_f). The ^{1}D Column was from SGE (Melbourne,
146 Australia) whereas the ^{2}D column was from Mega (Legnano, Milan, Italy).

147 The determination of the Linear Retention Indexes (I^T_S) on the first dimension was achieved by injecting 2
148 micro liters of the *n*-alkanes solution into the GC instrument with an Agilent ALS 7683B injection system.
149 The conditions used were the following: split/splitless injector, split mode, split ratio 1:50, injector
150 temperature 260°C.
151 Analytes were thermally desorbed from the SPME fiber into the GC injector for 10 min under the following
152 conditions: split/splitless in split mode, split ratio 1:20, injector temperature 260°C. The carrier gas was
153 helium, at a constant flow rate of 0.7 mL/min (initial head pressure 260 KPa). The oven temperature
154 program was: 50°C (1 min) to 170°C at 2.0°C/min and to 260°C at 50°C/min (10 min).
155 Data were acquired by an Agilent MSD ChemStation version D.02.00.275 and processed using GC Image
156 GC×GC Software version 2.1b1 (GC Image, LLC Lincoln NE, USA).
157
158 **2.6 HS-SPME-GC×GC-MS validation**
159 Method validation was run on a three-week protocol, over three-months, and the following parameters
160 were characterized: precision, linearity, accuracy, Limit of Detection (LOD) and Limit of Quantitation (LOQ).
161 Precision data (intra and inter-week precision on retention times and 2D Peak Volumes on analytes *Ti*) were
162 evaluated by replicating analyses during three months, while linearity was assessed through linear
163 regression analyses within the working range, over at least six different concentration levels and for each
164 quantification approach (i.e., SA and MHE). Experimental results on linearity assessment are in **Table 1**
165 (calibration ranges referred to analytes concentration in the matrix, regression curves and Determination
166 Coefficients R^2); precision is expressed as RSD% on analytes concentration, and is reported as Uncertainty %
167 in **Table 1**. Accuracy was assessed by cross-comparison of quantitative results obtained by SA and MHE
168 (correlation function) and through the absolute error.
169 The Limit of Quantification (LOQ) was determined experimentally by analyzing decreasing concentrations of
170 standard calibrating solutions in DBP by the MHE approach; each sample was analyzed in triplicate, and the
171 LOQ was the lowest concentration for which instrumental response (2D Peak Volume on *Ti*) reported an
172 RSD%, across replicate analyses, of below 30 %; for the Limit of Determination (LOD) the minimum
173 acceptable RSD% was set at 40%. LOD and LOQ are also reported in **Table 1**.

174 **3. RESULTS AND DISCUSSION**

175 **3.1 Quantitation challenges in headspace analysis**

176 The number of volatiles effectively contributing to the aroma of a food, i.e. the key odorants, is relatively
177 small, and complex analytical procedures are required to detect, identify, and quantify odor-active
178 components occurring at trace levels, in some cases below pg/g [12]. Exhaustive, classical approaches
179 based on liquid-liquid extraction, or more effective processes such as Solvent Assisted Flavour Evaporation
180 (SAFE), closely meet the needs of fundamental studies to isolate-identify-quantify key odorants [13], but
181 they are not compatible with high-throughput screenings, detailed profiling, and fast fingerprinting.

182 Headspace sampling (HS) plays a crucial role in this respect because it enables volatiles to be recovered
183 from the vapor phase, in equilibrium (or not) with the condensed (solid or liquid) phase of a sample, in a
184 process based on analytes' partition coefficients between matrix and vapor phase [11] and to analyze them
185 directly and on-line by GC×GC. HS performance can be implemented with the so-called High Concentration
186 Capacity Headspace Techniques (HCC-HS) [14], which are the elective route to satisfy headspace sampling
187 throughput and automation requirements, and that are useful to increase selectivity and sensitivity by
188 selecting appropriate sorbents/adsorbents suitable for the application need.

189 In particular, Solid Phase Microextraction (HS-SPME) [15] is the most widely-used HCC-HS technique; it is
190 based on multiple equilibria that are predictable, provided that a suitable number of analyte
191 physicochemical constants are known; it is also easy to standardize and to combine on-line or off-line with
192 the separation system.

193 Although quantitation by HS techniques is of great interest, only a limited number of food-volatile profiling
194 applications report data based on true quantitation [16-19], the common practice being cross-sample
195 comparisons through relative quantitation, based on Peak Area %, 2D Peak Volume % or Internal Standard
196 normalization. Although accepted by the scientific community for several application fields, these
197 approaches may result inaccurate [20,21] and misleading, if the aim of profiling and fingerprinting is to
198 correlate chemical composition and sensory properties, or process kinetics [9]. This consideration is of
199 special significance when a solid matrix is investigated.

200 The following sections will present some practical aspects of HS-SPME-GC×GC-MS quantitative chemical
201 profiling based on Multiple Headspace Extraction and on Standard Addition, together with a critical
202 discussion of the advantages, limits and versatility of each approach, in terms of the usability of data for
203 additional investigations based on an extended profiling of targeted and untargeted sample features.
204

205 **3.2 Quantitation strategies: experimental approach and data handling**

206 Two different approaches were evaluated and their performance parameters compared, taking into
207 consideration the challenging aspects of HS quantitation with solid samples, and the need to perform
208 detailed (untargeted and targeted) profiling and accurate targeted quantitation, contemporarily.
209 Standard Addition is a well-established approach, and was taken as reference technique for comparative
210 purposes, while Multiple Headspace Extraction, now receiving increasing attention in the food analysis field
211 [17,22-24], was chosen for its ability to provide rapid, reliable, and consistent quantitation of analytes, in
212 both matrix and the related headspace.
213 Quantitation was performed on a series of analytes present in the hazelnut volatile fraction, which are
214 highly informative for the aroma profile [25] and/or to qualify roasting treatment [2,26]. Nineteen analytes
215 were investigated: 2,3-pentanedione, hexanal, 1-methyl-1(H)-pyrrole, heptanal, pyridine, 2-methylpyrazine,
216 3-hydroxy-2-butanone, octanal, 5-methyl-(*E*)-2-hepten-4-one (filbertone), nonanal, *(E)*-2-octenal, 3-ethyl-
217 2,5-dimethylpyrazine, furfural, 2-ethyl-3,5-dimethylpyrazine, phenylacetaldehyde, *(E)*-2-decenal, 3-
218 methylbutanoic acid, 2-phenylethanol, and acetylpyrrole.
219

220 ***3.2.1 Standard Addition by HS-SPME-GC×GC-MS***

221 The standard addition procedure, widely used in headspace quantitation, consists of a series of
222 experiments in which the original sample, and a suitable number (at least six concentration levels) of
223 aliquots of the sample spiked with increasing and known amounts of reference compounds, are submitted
224 to the analytical process.
225 When using the single addition method, the analyte concentration in the sample can be estimated from
226 **Equation 1**:

227 $A_{(0+a)} = (A_0 / W_0)\, W_a + A_0$ **Eq.1**

228 where: W_0 is the amount of analyte in the matrix, W_a the amount of analyte added to the sample, A_0 the
229 instrumental response obtained from analysis of the original sample, and $A_{(0+a)}$ the instrumental response
230 of the analyte obtained from analysis of the spiked sample.

231 A preferable method, which was applied in this study, includes multiple standard additions, up to 6 levels;
232 in this case, a linear regression analysis evaluates the terms W_a and $A_{(0+a)}$ so that the amount of analyte in
233 the matrix (W_0) is given by the ratio between the intercept and the slope:

234 $b/a = A_0 / (A_0 / W_0)$ **Eq. 2**

235 SA is a quantitation approach that can be carried out in different ways: (*a*) by spiking the target analyte(s),
236 in a gaseous state, into the sample headspace (Gas Phase Addition - GPA); (*b*) by spiking the analyte(s)
237 dissolved in a suitable solvent, directly onto the sample (Sample Phase Addition - SPA) or (*c*) by spiking the
238 stable-isotope-labeled analyte(s) dissolved in a suitable solvent (Stable Isotope Dilution Analysis - SIDA)
239 onto the sample. This study adopted the Sample Phase Addition protocol, as being suitable for its ease of
240 implementation and automation, and its cost, despite its limits with solid matrix samples (ground
241 hazelnuts) and the resulting well-known matrix effect. In particular, the selection of an appropriate solvent
242 for spiking solutions, and the possibility to suspend ground particles in water to minimize concurrent
243 adsorption/sorption of analytes, were investigated. A series of experiments (data not shown) indicated that
244 dibutyl phtalate (DBP) guarantees full solubilization of all the target analytes, homogeneous dispersion of
245 the spiked volumes, and absence of interfering compounds, that were detected in the other lipophilic
246 media tested (sunflower oil and degassed oleic fraction of vegetable fats).

247

248 ***3.2.2 Multiple Headspace Extraction by HS-SPME-GC×GC-MS***

249 MHE was applied as External Standard quantitation approach; it consists of two experimental steps:
250 (*a*) exhaustive extraction of representative samples and method calibration, and (*b*) real-world sample
251 analysis. The first step aims to define a cumulative instrumental response function, through a series of
252 repeated and consecutive extractions of appropriate amounts of the same sample from the headspace, up
253 to complete (exhaustive) extraction of the analytes under study.

254 The analyte peak area/volume decreases exponentially with the number of extractions, while the partition
255 coefficient (*K*) between the matrix and the headspace remains constant, provided headspace linearity is
256 achieved [11]. The sum of the areas from each extraction step corresponds to the total area (A_T) of the
257 analyte originally present in the matrix. The cumulative instrumental response is obtained from **Equation 3**:

258 $$A_T = \sum_{i=1}^{=\infty} A_i = A_1 \frac{1}{\left(1-e^{-q}\right)} = \frac{A_1}{(1-\beta)}$$ **Eq. 3**

259 where A_T is the total estimated area, A_1 is the area detected after the first extraction, and *q* is a constant
260 describing the exponential decay of the area with successive extractions. The term *q* can be obtained by
261 plotting the logarithm of chromatographic areas as a function of the number of extractions. From this, a
262 linear regression equation can be calculated as $y=ax+b$, where $y = \ln A_i$, $x=(i-1)$, *b* is the intercept on the *y*
263 axis, and *a* is the slope.
264 The value of β is in general constant (or, at least, within an acceptable range fixed *a priori*) for each
265 quantified analyte, if calculated in a series of relatively homogeneous representative samples of the same
266 matrix, i.e. samples showing comparable matrix effect [24 and references cited therein]. The same
267 procedure, repeated in parallel with a standard mixture at different known concentrations (six calibration
268 points covering the expected concentration range in the sample), enables an external calibration curve to
269 be built up. Under these conditions, the calibration curve can be used to determine the analyte amount in
270 the sample, from its area obtained from a single analysis.The second step, application of MHE to real-world
271 samples of the same matrix, does not require further experiments, unless different matrix effects from
272 those of the representative samples used in the training set (resulting in different *β* values) are produced.
273 Experiments on hazelnuts from different geographical origins and that had undergone different thermal
274 processing showed that they had comparable matrix effects, resulting in a very limited dispersion of β
275 values (**Table 2**), as expected on the basis of the distribution of primary and secondary metabolites in the
276 nuts (lipids, proteins, soluble carbohydrates and fiber). The same applied to *Gianduja* paste from different
277 manufacturers, although, as expected, they were different from that of ground hazelnuts (**Table 3**). This
278 difference is negligible in term of quantitation accuracy with the MHE approach, but it is a limit for SA on

279 solids, where partition/equilibration of spiked analytes takes time and requires appropriate
280 homogenization and equilibration before sampling, prior to calibration.
281 The following paragraphs report quantitative results and method performance parameters, while critically
282 discussing the potentials and limits of each approach from the perspective of exhaustive volatiles
283 assessment (profiling and fingerprinting).
284
285 **3.3 Quantitation Results**
286 **Table 4** summarizes quantitation results, obtained by MHE, on key odorants and technological markers for
287 hazelnuts (*Tonda Gentile* and *Ordu*) at two commercially-applied degrees of roasting, while **Table 5** reports
288 results for *Gianduja* paste with different formulations (Samples #1 to #4) and manufacturers (Samples #1-4
289 and #5); data are expressed as ng/g in the original product.
290 The results on hazelnuts, from both approaches, are consistent with those recently published by Kiefl *et al*
291 [27], which were obtained with a well-established technique, i.e. Stable Isotope Dilution Analysis (a
292 Standard Addition approach) on Solvent Assisted Flavor Evaporation extracts from hazelnut.
293 Mild roasting produces lower concentrations of both key odorants and technological markers, and different
294 cultivars perform differently, as was expected on the basis of previous studies [28]. Roasting markers (3-
295 hydroxy-2-butanone and furfural) required an extended calibration interval, while several key odorants in
296 mildly roasted products fell below the method LOQ ((*E*)-2-octenal and (*E*)-2-decenal).
297 For *Gianduja* paste, the results are relatively uniform, the first four samples being formulation tests from
298 the same manufacturer, with minimal changes in the main ingredients (sugar, fats of vegetable origin,
299 hazelnut paste, cocoa, nonfat dry milk), while Sample #5 was a commercial product (made by a different
300 manufacturer) purchased in a local supermarket. The distribution of analytes consistently followed the
301 profile of roasted hazelnuts, although with marked differences due to their concurrent presence in the
302 other ingredients, such as cocoa, fats and vanilla flavoring.
303 Several observations can be drawn from the method performance parameters. Firstly, both SA and MHE
304 methods showed good consistency in quantification results between roasting batches (#1 and #2) (data not
305 shown), confirming that lab-scale roasting is reproducible and provides consistent results for model studies

306 [4]. Secondly, MHE performs better than SA in terms of precision; Relative Standard Deviation % (RSD %) on
307 replicated determinations (n=3) over the two batches (for a total of six quantifications) remain below 20%
308 with few exceptions (50.5 % for hexanal in *Ordu 170-35* and 36.7 % for the 2-ethyl-3,5-dimethylpyrazine in
309 *Ordu 170-20*). One-Way ANOVA, applied to the quantitative results for the two batches from three
310 replicate extractions for MHE, or spiked aliquots for SA, showed (95% interval of confidence) that a single
311 cumulative RSD% value can be adopted to describe intermediate precision as major contributor to
312 quantitation uncertainty (reported as Relative Uncertainty % for each method in **Table 1**).
313 Linearity was evaluated by running multiple extractions (in triplicate) on increasing concentrations of
314 analyte standard calibrating solutions in DBP, within the working interval (MHE), and on spiked aliquots (in
315 triplicate) of roasted hazelnuts (SA). The average values of instrumental response (expressed as *Ti*
316 Normalized Peak Volume) recorded over at least six calibration levels were used for linear regression
317 analyses, and linearity was evaluated by calculating the coefficient of determination (R^2).
318 Results referred to the *Ordu 170-35* sample for SA, and to the cumulative response of calibrating solutions
319 in DBP within the working interval for MHE, are reported in **Table 1** and show very good linearity, with an
320 average R^2 value of 0.975 for SA, and 0.978 for MHE. Accuracy was verified by regression analyses on
321 quantitative data obtained by SA and MHE, results for selected samples (*TGT 170-35* and *Ordu 170-35*) are
322 shown in **Figure 1** and indicate appropriate performances (R^2= 0.966). There was an increased
323 quantification error for linear aldehydes, *(E)*-2-octenal and *(E)*-2-decenal, and furfural, due to greater
324 dispersion of the results (RSD above 25%) from SA. These exceptions were expected, because of the critical
325 re-equilibration of spiked aldehyde standards, also reported in other studies [23]; for furfural, the
326 quantification error in SA was caused by its wide concentration range in the samples studied.
327

328 **3.4 Additional information provided by Multiple Headspace Extraction**

329 The quali-quantitative composition of the vapor phase that reaches the *regio olfactoria* through retronasal
330 and/or orthonasal pathways is extremely informative of the sensory characteristics of a food. This is
331 confirmed by the ever-increasing interest in developing fast, non-invasive, sensitive, and highly specific
332 methods for monitoring volatiles in real-time, during food consumption [29,30]. Conversely, recent studies

333 on wine aroma [23] report significant differences in liquid-gas transfer rates of key odorants from wines,
334 which exert different matrix effects due to their specific compositions. For instance, the presence of sulfur
335 dioxide decreases the release of carbonyl compounds, while polyphenols and tannins may reduce the gas-
336 phase distribution of alcohols [23]. In this respect, a suitable investigation strategy is necessary to establish
337 the absolute concentration of key analytes, both in the matrix itself and in the headspace, to reveal the
338 aroma and the technological blueprint of a product [31].
339 Multiple Headspace Extraction offers the possibility to evaluate both aspects contemporarily; β values and
340 the logarithmic decrease of analyte chromatographic area, along with successive extraction steps, provide
341 information about their relative release into the headspace and their distribution in the solid matrix.
342 **Figure 2** shows the different behaviors of three key odorants:5-methyl-(*E*)-hepten-4-one (filbertone), 2-
343 ethyl-3,5-dimethylpyrazine and 2-phenylethanol. The graph is based on equal terms of cumulative response
344 (A_T), arbitrarily fixed at 100 counts for comparative purposes. The red and black lines depict the logarithmic
345 decay of analytes from calibration solutions in DBP-*red* and in cyclohexane-*black* (corresponding to
346 calibrants in the gas phase approach); filbertone apparently does not present significant partition with DBP,
347 whereas partition for 2-ethyl-3,5-dimethylpyrazine and for 2-phenylethanol were significant. The blue and
348 green lines indicate analyte behavior in hazelnuts and in the *Gianduja* paste; in this case, a comparable
349 matrix effect is evident (β values are close to one another) with a general tendency of the matrix to retain
350 analytes (higher partition coefficients), delaying their release into the headspace.
351 As recently shown by Ferreira *et al.* [23], MHE enables the pseudo distribution constant (*K*) to be estimated,
352 giving analyte mass ratio between headspace (C_G) and condensed-phase (C_0), and thus providing a
353 quantitative indication of the average compound mass transferred to volume units of headspace per
354 concentration unit of compound remaining in the condensed phase. This information can be useful to
355 evaluate the different release rates of key odorants from food formulae that differ for their actual matrix
356 effect and/or to optimize doses of flavorings.
357 In the present study, interesting evidence was revealed by comparing β values of a set of analytes from
358 different matrices (real-world samples, DBP and cyclohexane) at the same temperature and headspace
359 volume. Within the selected targets, less volatile analytes with vapor pressure values below unity (i.e. 2-

360 ethyl-3,5-dimethylpyrazine, 3-methylbutanoic acid, (*E*)-2-octenal, nonanal, phenylacetaldehyde,
361 acetylpyrrole, 2-phenylethanol and (*E*)-2-decenal) showed marked differences between MHE β values in
362 gas phase and those estimated in lipophilic media (DBP) and in real-world samples (cf. **Table 1**). For these
363 analytes, a crucial role is played in their release from the food matrix by partition, rather than by volatility.
364 Conversely, high-volatility components with vapor pressure values above 10 (i.e., 2,3-pentanedione, 1-
365 methyl-1(H)-pyrrole, pyridine and hexanal) showed a negligible partition effect in DBP, and higher retention
366 in hazelnut samples, where solid particles presumably exert absorption phenomena.
367
368 **3.5 Detailed profiling and quantitative fingerprinting**
369 The results obtained from the above experiments are fundamental for further advancements on profiling
370 and fingerprinting analysis based on 2D pattern similarity for sample comparison and classification. In
371 particular, markers involved with geographical origin and technological treatment of roasted hazelnuts are
372 here investigated [19,20]. The *Comprehensive Template Matching* fingerprinting approach is here applied:
373 it establishes consistent correspondences for all the untargeted peaks with coherent retention times and
374 whose fragmentation pattern referred a fixed degree of similarity with a corresponding template spectrum.
375 The higher the number of consistent features compared across samples is, the higher specificity and
376 sensitivity of the process are. The possibility to perform a simultaneous targeted quantitative assessment
377 on selected informative peaks and an extended untargeted screening over the complete 2D peak pattern is
378 a key-aspect to extend the informative potential of GC×GC-MS.
379 MHE offers the possibility to approach both investigation steps, although some limits may arise from the
380 amount of processed sample, that must give adequate decay through successive extractions. Only analytes
381 whose concentrations in sample (C_0) and headspace (C_G) follow a linear relationship, generally
382 corresponding to concentrations below 0.1-1%, can adequately be quantified [11].
383 Four different aliquots (i.e., 1.500, 1.000, 0.500 and 0.100 g) of *Tonda Gentile Trilobata* (*TGT 170-35*) were
384 sampled by HS-SPME, to test the feasibility of overall assessment of volatiles, the resulting volatiles were
385 analyzed by GC×GC-MS and peak features from each pattern collected in a *Consensus template.* The
386 template consisted of *335* 2D peaks, with *137* known and *198* unknowns. Analytes were identified on the

387 basis of their linear retention indexes and MS-EI spectra compared with those of authentic standards (when
388 available) or tentatively identified through their MS-EI fragmentation patterns and retention indexes. The
389 list of peak features (i.e. Compound Name, ^{1}D Retention time (min), ^{2}D Retention time (sec), ^{1}D Linear
390 Retention Index (I^{T}_{S}), Normalized 2D Peak Volume, and Reference MS) is provided as a supplementary table
391 (**Supplementary Table ST1**) while **Figure 3** summarizes the results, together with the 2D peak patterns
392 obtained by analyzing the different aliquots. As may be seen, the number of matched peaks within the set
393 of chromatograms (average 3 replicate analyses) decreased, from 100% with the 1.500 g sample to 73%
394 with the 0.100 g sample, the latter corresponding to the sample amount for which target analytes
395 submitted to MHE quantitation showed a linear response. More precisely, 73 unknown and 17 known
396 analytes were lost by sampling 0.100 g; within the group of targets; only a few odor-active compounds, and
397 one key aroma compound (i.e., 2-acetyl-1-pyrroline) fell below the method LOD; other informative
398 features, discriminating botanical and geographical origins, as well as the extent of technological treatment
399 [17,22,23], were consistently matched, thus providing detailed profiling.
400 In addition, untargeted features, whose decay along through successive extraction steps demonstrates
401 adequate linearity, could be investigated in terms of actual release from the sample matrix through their β
402 value, and additional information on their extraction rate added to the global assessment, as shown in
403 **Figure 4** for the compounds trimethylpyrazine, furfuryl alcohol, and 2,5-dimethyl-4-hydroxy-3(2H)-
404 furanone. In the example given, the first two compounds, characterized by faster decay, would be more
405 rapidly released into the headspace than would 2,5-dimethyl-4-hydroxy-3(2H)-furanone (furaneol™). The
406 latter, being a key odorant in roasted hazelnuts, although not quantified in the present study, provides
407 further information on sample sensory quality. It should be stressed that the sensitivity of GC×GC plays a
408 crucial role for these investigations, which cannot, with comparable effectiveness, be achieved by one-
409 dimensional approaches, because of the higher LODs that can be achieved with the latter.
410

411 **4. CONCLUSIONS**

412 The study presents a successful investigation strategy implemented on a "comprehensive" analytical
413 platform; in particular, the advantages of quantitative headspace analysis are discussed from the

414 perspective of a complete and informative assessment of complex food sample volatiles. Emphasis is
415 placed on the potential of each analytical step in term of the dimensionality of the information provided.
416 Thus also sample preparation by HS-SPME is included, as is separation by GC×GC, detection by EI-MS and
417 data elaboration by advanced fingerprinting approaches [2,33].
418 In order to be considered as a further dimension of the analysis system, HS-HCC sampling techniques, and
419 in particular HS-SPME, are the key step to provide a consistent (quantitative aspects) and meaningful
420 (qualitative aspects) picture of the sample/fraction under study. Experiments carried out on food volatile
421 fractions demonstrate that the information potential of each analysis can better be exploited, thanks to: (*a*)
422 the method's adoption of multiple and orthogonal extraction principles (adsorption and sorption)
423 combined on the SPME fiber, (*b*) the minimization of artifact formation, by keeping sampling temperature
424 and time controlled, (*c*) the headspace linearity conditions applied, and (*d*) the adoption of versatile and
425 reliable quantitation protocols (in particular MHE).
426 A crucial role is undoubtedly played by the separation technique adopted; GC×GC provides detailed
427 profiling of volatiles even when the sample matrix to be analyzed must be reduced tenfold or more, to
428 comply with quantitation requirements, thanks to its high selectivity and efficiency, due to the orthogonal
429 combination of separation mechanisms, and also to its sensitivity, which is achieved by appropriate column
430 selection.
431 The two quantitation methods applied were found to be adequate for accurate quantitative determination
432 of the selected target analytes in the sample matrix (with the exception of aldehydes for SA), but revealed
433 different aptitudes, in terms of information potential and ease of execution. In particular, MHE was more
434 versatile, providing information on the sample matrix effect, which is important to evaluate the release of
435 volatiles from the food matrix, and on their relative distribution between gas and condensed phases. MHE
436 carried out with an External Standard approach does not requires equilibration or partition of spiked
437 analytes, which is the critical step of SA for solid samples; further, it also makes possible concurrent
438 quantitative investigation of the complete set of selected volatiles.
439 The present strategy is a useful approach from the perspective of sensomics and flavoromics, since it
440 comprises an integrated analytical platform able to provide information on the qualitative and quantitative

441 distribution of sensory active compounds, through a fully-integrated system including multiple dimensions
442 of analysis: sample preparation-separation-identification/quantitation-advanced data elaboration.
443

444 **Acknowledgements**

445 This research was carried out within the “ITACA” and “ECOFOOD” projects of the POR-FESR “Competitività
446 regionale e occupazione” 2007/2013, Asse 1, Misura I.1.1, “Piattaforme innovative” of the Piedmont Region
447 (Italy).
448

449 **References**

450 [1] http://ec.europa.eu/agriculture/quality/schemes/index_en.htm Accessed 11.06.2013
451 [2] C. Cordero, E. Liberto, C. Bicchi, P. Rubiolo, S. E. Reichenbach, X. Tian, Q. Tao, J. Chrom. Sci. 48
452 (2010)251-261.
453 [3] C. Cagliero, C. Bicchi, C. Cordero, P. Rubiolo, B. Sgorbini, E. Liberto, Food Chem. 132 (2012) 1071-1079.
454 [4] L. Nicolotti, C. Cordero, C. Bicchi, P. Rubiolo, B. Sgorbini, E. Liberto, Food Chem. 138 (2013) 1723-1733.
455 [5] C. Cordero, E. Liberto, C. Bicchi, P. Rubiolo, P. Schieberle, S. E. Reichenbach, Q. Tao, J. Chromat. A. 1217
456 (2010) 5848-5858
457 [6] S. G. Oliver, M. K. Winson, D. B. Kell, F. Baganz, Trends Biotechnol. 16(1998) 373-381
458 [7] C. H. R. de Vos, Y. Tikunov, A. G. Bovy, R. D. Hall. In Expression of Multidisciplinary Flavour Science. I.
459 Blank, M. Wust, C. Yeretzian (eds.). Proceedings of the 12th Weurman Symposium, Zürcher Hochschule für
460 Angewandte and Institut Für Chemie und Biologische Chemie, Interlaken, Switzerland, 2008, pp. 573–580
461 [8] M. Herrero, C. Simõ, V. García-Cañas, E. Ibáñez, A. Cifuentes, Mass Spectrom. Rev. 31 (2012) 49-69.
462 [9] J. Kiefl, G. Poller, P. Schieberle, J. Agric. Food Chem, DOI: 10.1021/jf400807w
463 [10] J. Charve J, C Chen, A. D. Hegeman, G. A. Reineccius, Flavour Frag. J. 26 (2011) 429-440.
464 [11] B. Kolb, L.S Ettre, Static Headspace-Gas Chromatography, Theory and Practice. Wiley-VCH, New York,
465 1997.
466 [12] W. Grosch, Chem Senses 26 (2001) 533-545

[13] R.G. Berger, Flavours and Fragrances: Chemistry, Bioprocessing and Sustainability, Springer-Verlag Berlin, 2007.

[14] C. Bicchi, C. Cordero,E. Liberto, B. Sgorbini, P. Rubiolo, J. Chromatogr. A. 1184 (2008) 220-233.

[15] J. Pawliszyn, Solid Phase Microextraction - Theory and Practice, Wiley-VCH: New York, 1997

, J. Chromatogr. A. 1216 (2009) 127-133.

[17] R. Costa, L. Tedone, S. De Grazia, P. Dugo, L. Mondello, Anal. Chim. Acta. 770(2013) 1-6

[18] R.R. Jetti, A.Kurnianta, C. Finn, M.C. Qian, J. Food Sci. 72 (2007) 487-496.

[19] R. Natera Marın, R. Castro Mejìas , M. de Valme Garcia Moreno,F. Rowe, C. Garcia-Barroso, J. Chromatogr. A. 967 (2006) 261-267. [20] C. Bicchi,1 E. Liberto, M. Matteodo, B. Sgorbini, L. Mondello, B. d'Acampora Zellner, R. Costa, P.Rubiolo, Flavour Fragr. J. 23 (2008) 382-391.

[21] J.Y. De Saint Laumer, E Cicchetti, P-Merle, J. Egger, A. Chaintreau, Anal. Chem. 82 (2010) 6457–6462

[22] A. N. Birch, M. A. Petersen, A. S. Hansen, Food Sci. Tech. 50 (2013) 480-488.

[23] J. Zapata, R. Lopez, P. Herrero, V. Ferreira, J. Chromatogr. A. 1266 (2012) 1-9.

[24] C. Bicchi, M. R. Ruosi, C. Cagliero, C. Cordero, E. Liberto, P. Rubiolo, B. Sgorbini, J. Chromat. A. 1218 (2011) 753-762.

[25] A.Burdack Freitag, P. Schieberle, J. Agric. Food Chem.60 (2012) 5057-5064

[26] C. Cordero, E. Liberto, C. Bicchi, P. Rubiolo, P. Schieberle, S. E. Reichenbach, Q. Tao, J. Chromat. A. 1217 (2010) 5848-5858

[27] J. Kiefl, P. Schieberle, J. Agric. Food Chem. DOI: 10.1021/jf4008086

[28] J. Kiefl, C. Cordero, L. Nicolotti, P. Schieberle, S. E. Reichenbach, C. Bicchi, J. Chromatogr. A. 1243 (2012) 81-90.

[29]F. Biasioli, F. Gasperi., C. Yeretzian, T.D. Märk, J. Dewulf, H. R.Van Langenhove,TrAcs. 30 (2011) 968-977.

[30] S. J. Avison, J. Agric. Food Chem.61 (2013) 2070-2076

[31] M. Christlbauer, P. Schieberle, J. Agric. Food Chem. 57 (2009) 9114-9122

[32] C. Cordero, C. Bicchi, P. Rubiolo, J. Agric. Food Chem. 56 (2008) 7655-7666

[33] S.E. Reichenbach, X. Tian, C. Cordero, Q. Tao, J. Chromatogr. A.1226 (2012) 140-148

494 **Caption to Figures**

495 **Figure 1**: Results of accuracy assessment. Regression analysis on estimated concentrations for target
496 analytes (ng/g) in TGT 170-35 and Ordu 170-35 samples. Outliers (linear and unsaturated aldehydes and
497 furfural) are excluded.
498
499 **Figure 2**: MHE slopes (β) for selected target analytes (5-methyl-*(E)*-2-hepten-4-one, 2-ethyl-3,5-
500 dimethylpyrazine and 2-phenylethanol). The graphs are based on equal terms of cumulative response (A_T)
501 arbitrarily fixed at 100 counts. Red and black lines show the logarithmic decay from calibration solutions in
502 DBP-red and in cyclohexane-black (corresponding to calibrants in the gas phase approach) whereas blue
503 and green lines indicate analyte behavior in hazelnuts and in the Gianduja paste, respectively.
504
505 **Figure 3**: HS-SPME-GC×GC-MS patterns from different aliquots of TGT 170-35 together with fingerprinting
506 results: Number of template peaks present in the *consensus template* (see text for details), Number of
507 reliably matched peaks, % of matching, and identity of unmatched target peaks. Key odorants are
508 underlined.
509
510 **Figure 4:** MHE slopes (β) for selected analytes not included in the pool of quantified targets.
511

512 **Caption to Tables**

513 **Table 1**: List of target analytes considered in the quantitative fingerprinting, together with their CAS
514 Registry Number, Purity % of the reference compound used for calibration, calculated physicochemical
515 properties (Vapor Pressure – Vp and octanol/water partition coefficient – LogP), Target Ion and Qualifiers
516 adopted for quantitation. Validation parameters include: calibration ranges (ng/g), regression curves for SA
517 and MHE calculated over six calibration points, coefficients of determination (R^2), Uncertainty % (Unc.%),
518 Limit of Determination (LOD) and Limit of Quantitation (LOQ). See text for details.
519
520 **Table 2**: Multiple Headspace Extraction calibration parameters. β values and coefficients of determination
521 (R^2) for target analytes in hazelnut samples differing for geographical origins (Tonda Gentile Trilobata TGT
522 and Ordu) and roasting conditions. The two right-hand columns report calibration slopes in different media:
523 Dibutyl Phtalate DBP and Cyclohexane (equivalent to Gas Phase).
524
525 **Table 3**: Multiple Headspace Extraction calibration parameters. β values and coefficients of determination
526 (R^2) for target analytes in *Gianduja* samples differing in formulation and manufacturer (Samples # 1-4 and
527 Sample #5, respectively). The two right-hand columns report average values and precision (Relative
528 Standard Deviation %).
529
530 **Table 4**: MHE quantitation results of hazelnut samples for accuracy assessment. Concentration is expressed
531 in ng/g in the matrix, precision data is referred to replicate determination over three months (see text for
532 validation details).
533
534 **Table 5**: MHE quantitation results in *Gianduja* paste. Concentration and corresponding uncertainty are
535 expressed in ng/g in the matrix (see text for details).

Table 1

								Standard Addition			Multiple Headspace Extraction				
ID	**Compound name**	**CAS RN**	**Purity**	**Vp[a] (Torr, 25°C)**	**Log P[b]**	***Target Ion* Qualifiers**	**Calibration range (ng/g)**	**Regression curve (n=6)**	**R^2**	**Unc.%**	**Regression curve (n=6)**	**R^2**	**Unc.%**	**LOD ng/g**	**LOQ ng/g**
1	2,3-pentanedione	600-14-6	97%	26.40	-0.831±0.297	*43*, 57, 100	10-2500	y = 3700.7x + 188647	0.991	10.8	y = 8015.6x + 37875	0.948	9.6	9.45	50.56
2	hexanal	66-25-1	98%	10.90	1.932±0.223	*44*, 56, 82	10-1500	y = 2642x + 297645	0.969	29.1	y = 5856.7x + 120348	0.999	15.0	2.60	11.48
3	1-methyl-1(H)-pyrrole	96-54-8	98%	25.60	1.351±0.251	*81*, 80, 53	10-1500	y = 567.92x + 39891	0.993	10.3	y = 1047.2x - 21952	0.974	10.5	12.19	51.89
4	heptanal	111-71-7	92%	3.85	2.442±0.223	*44*, 70, 55	10-1500	y = 967.76x + 58880	0.923	14.6	y = 2683.4x + 4197.7	0.999	5.0	1.12	5.64
5	pyridine	110-86-1	98%	22.80	0.836±0.178	*79*, 52, 51	10-1500	y = 821.45x + 49360	0.993	9.8	y = 2021x - 36590	0.979	2.1	10.58	50.34
6	2-methylpyrazine	109-08-0	99%	9.69	0.342±0.236	*94*, 67, 53	100-2500	y = 5582.8x + 989884	0.947	5.8	y = 14211x - 103899	0.997	5.6	5.02	22.36
7	3-hydrox-2-butanone	513-86-0	96%	1.92	-0.299±0.287	*45*, 43, 88	100-2500	y = 1772.9x + 195105	0.984	23.5	y = 16032x - 241081	0.955	6.7	2.22	11.21
8	5-methyl-(*E*)-2-hepten-4-one	102322-83-8	98%	1.25	2.023±0.252	*69*, 98, 111	100-2500	y = 10184x + 721440	0.997	9.5	y = 24400x - 62922	0.983	9.7	2.05	10.36
9	octanal	124-13-0	99%	2.07	2.951±0.223	*43*, 56, 84	10-1500	y = 1045.3x + 61668	0.993	11.5	y=2343.7x - 29123	0.978	5.4	6.24	27.58
10	nonanal	124-19-6	95%	0.53	3.461±0.223	*57*, 41, 70	10-4000	y = 1590.5x + 142268	0.981	63.6	y = 3339.4x + 5118.2	0.993	5.5	0.23	0.91
11	(*E*)-2-octenal	2548-87-0	94%	0.55	2.809±0.282	*41*, 55, 70	100-2500	y = 1582.3x + 23986	0.995	13.1	y = 6291.8x - 91734	0.953	7.1	11.45	49.46
12	3-ethyl-2,5-dimethylpyrazine	13360-65-1	98%	1.21	1.457±0.318	*135*, 136, 108	10-1500	y = 622.15x + 67165	0.966	6.1	y = 3596.5x + 68708	0.999	4.5	0.38	1.50
13	furfural	98-01-1	99%	2.23	0.712±0.264	*96*, 95, 39	100-10000[c]	y = 5694.8x + 3E+06	0.998	7.6	y = 12439x - 72625	0.989	5.5	6.10	24.46
14	2-ethyl-3,5-dimethylpyrazine	13925-07-0	98%	0.81	1.457±0.318	*135*, 136, 108	10-1500	y = 1225.6x + 25489	0.941	11.7	y = 4537x + 1419.7	0.974	18.8	0.37	0.90
15	phenylacetaldehyde	122-78-1	95%	0.37	1.760±0.224	*91*, 120, 65	10-1500	y = 3996.1x + 75391	0.986	12.3	y = 15521x - 362929	0.987	11.5	5.73	25.55
16	(*E*)-2-decenal	3913-81-3	92%	0.07	3.828±0.282	*41*, 55, 70	10-1500	y = 77.653x + 2728	0.941	7.9	y = 3324.4x - 68279	0.975	5.0	4.70	23.57
17	3-methylbutanoic acid	503-74-2	99%	0.55	1.051±0.193	*60*, 74, 87	10-1500	y = 2653x + 50140	0.991	15.5	y = 12958x - 242712	0.959	5.6	1.75	5.28
18	2-phenylethanol	60-12-8	98%	0.07	1.504±0.186	*91*, 122, 65	10-1500	y = 1886.7x + 14875	0.971	14.7	y = 20548x - 136118	0.971	2.8	5.47	24.36
19	acetylpyrrole	1072-83-9	99%	0.11	0.911±0.312	*94*, 109, 66	10-1500	y = 1188.7x + 55489	0.957	4.9	y = 11349x - 166508	0.974	7.2	1.59	5.35

[a,b]: Calculated using Advanced Chemistry Development (ACD/Labs) Software V11.02 (© 1994-2013 ACD/Labs)(Toronto, ON, Canada)

[c]: calibration was performed in two intervals (100-2500 and 2500-10000)– MHE and SA calibration curves reported are referred to 100-2500 ng/g

Table 2

		TGT 170-20		TGT 170-35		Ordu 170-20		Ordu 170-35		Summary		Calibration slopes	
ID	**Compound name**	**β**	**R^2**	**β**	**R^2**	**β**	**R^2**	**β**	**R^2**	**β av**	**RSD%**	**β_{DBP}**	**β_{GP}**
1	2,3-pentanedione	0.67	0.979	0.76	0.995	0.61	0.935	0.66	0.979	0.62	9.00	0.42	0.39
2	hexanal	0.70	0.998	0.71	0.929	0.54	0.987	0.65	0.964	0.66	8.69	0.31	0.32
3	1-methyl-1(H)-pyrrole	0.63	0.981	0.77	0.971	0.55	0.909	0.60	0.889	0.57	12.44	0.19	0.13
4	heptanal	0.58	0.884	0.56	0.997	0.57	0.962	0.65	0.989	0.60	6.13	0.19	0.18
5	pyridine	0.45	0.989	0.50	0.959	0.39	0.908	0.51	0.973	0.48	12.72	0.48	0.50
6	2-methylpyrazine	0.62	0.901	0.63	0.982	0.52	0.979	0.62	0.995	0.60	9.32	0.21	0.19
7	3-hydrox-2-butanone	0.70	0.945	0.87	0.929	0.72	0.950	0.89	0.967	0.79	9.93	0.65	0.75
8	5-methyl-(*E*)-2-hepten-4-one	0.64	0.994	0.76	0.969	0.69	0.987	0.70	0.997	0.70	6.39	0.23	0.21
9	octanal	0.77	0.926	0.66	0.906	0.67	0.927	0.80	0.992	0.70	8.54	0.15	0.12
10	nonanal	0.81	0.904	0.85	0.929	0.82	0.925	0.63	0.767	0.80	10.36	0.48	0.31
11	(*E*)-2-octenal	< LOD	-	< LOD	-	0.95	0.988	0.83	0.914	0.84	14.46	0.41	0.26
12	3-ethyl-2,5-dimethylpyrazine	0.86	0.993	0.87	0.983	0.60	0.963	0.92	0.903	0.82	14.18	0.40	0.19
13	furfural	0.61	0.975	0.70	0.985	0.66	0.976	0.74	0.995	0.68	8.45	0.11	0.09
14	2-ethyl-3,5-dimethylpyrazine	0.74	0.936	0.88	0.948	0.76	0.969	0.90	0.948	0.81	11.05	0.44	0.22
15	phenylacetaldehyde	0.90	0.932	0.80	0.998	0.79	0.992	0.79	0.967	0.83	5.52	0.49	0.23
16	(*E*)-2-decenal	< LOD	-	< LOD	-	0.79	0.992	0.79	0.954	0.82	5.72	0.76	0.26
17	3-methylbutanoic acid	0.90	0.982	0.85	0.904	0.66	0.987	0.85	0.974	0.82	9.27	0.57	0.81
18	2-phenylethanol	0.90	0.932	0.89	0.957	0.89	0.998	0.88	0.980	0.85	6.71	0.79	0.33
19	acetylpyrrole	0.86	0.990	0.92	0.993	0.88	0.992	0.95	0.899	0.89	7.21	0.77	0.31

Table 3

		Sample #1		Sample #2		Sample #3		Sample #4		Sample #5			
ID	**Compound name**	**β**	**R^2**	**β**	**R^2**	**β**	**R^2**	**β**	**R^2**	**β**	**R^2**	**β av**	**RSD%**
1	2,3-pentanedione	< LOQ	-	< LOQ	-	< LOQ	-	< LOQ	-	< LOQ	-	-	-
2	hexanal	0.81	0.988	0.77	0.982	0.79	0.966	0.85	0.954	0.83	0.996	0.81	3.88
3	1-methyl-1(H)-pyrrole	< LOQ	-	< LOQ	-	< LOQ	-	< LOQ	-	< LOQ	-	-	-
4	heptanal	0.58	0.985	0.38	0.848	0.49	0.971	0.44	0.958	0.60	0.879	0.54	12.65
5	pyridine	0.59	0.994	0.28	0.822	0.28	0.822	0.48	0.985	0.48	0.989	0.42	12.26
6	2-methylpyrazine	0.66	0.961	0.56	0.974	0.80	0.982	0.74	0.978	0.52	0.933	0.66	12.63
7	3-hydrox-2-butanone	0.86	0.976	0.65	0.992	0.90	0.925	0.82	0.963	0.62	0.956	0.81	9.19
8	5-methyl-(*E*)-2-hepten-4-one	0.59	0.999	0.51	0.962	0.51	0.985	0.58	0.984	0.63	0.967	0.56	9.06
9	octanal	0.53	0.851	0.53	0.851	0.60	0.979	0.69	0.984	0.81	0.974	0.61	13.85
10	nonanal	0.76	0.809	0.32	0.940	0.77	0.859	0.78	0.962	0.78	0.962	0.76	3.29
11	(*E*)-2-octenal	< LOQ	-	< LOQ	-	< LOQ	-	< LOQ	-	< LOQ	-	-	-
12	3-ethyl-2,5-dimethylpyrazine	0.60	0.910	0.60	0.944	0.66	0.886	0.72	0.993	0.86	0.953	0.67	10.57
13	furfural	0.71	0.953	0.57	0.930	0.58	0.945	0.53	0.996	0.53	0.978	0.58	12.35
14	2-ethyl-3,5-dimethylpyrazine	0.54	0.928	0.78	0.989	0.72	0.999	0.72	0.993	0.83	0.929	0.74	9.69
15	phenylacetaldehyde	< LOQ	-	< LOQ	-	< LOQ	-	< LOQ	-	< LOQ	-	-	-
16	(*E*)-2-decenal	< LOQ	-	< LOQ	-	< LOQ	-	< LOQ	-	< LOQ	-	-	-
17	3-methylbutanoic acid	0.81	0.981	0.49	0.930	0.63	0.982	0.69	0.978	0.69	0.994	0.66	7.75
18	2-phenylethanol	0.92	0.966	0.49	0.844	0.87	0.998	0.88	0.993	0.75	0.962	0.84	8.25
19	acetylpyrrole	0.84	0.976	0.74	0.935	0.78	0.990	0.84	0.982	0.70	0.985	0.78	7.82

Table 4

		TGT 170-20 conc (ng/g)				TGT 170-35 conc (ng/g)				ORDU 170-20 conc (ng/g)				ORDU 170-35 conc (ng/g)			
ID	**Compound name**	**SA**	**RSD%**	**MHE**	**RSD%**	**SA**	**RSD%**	**MHE**	**RSD%**	**SA**	**RSD%**	**MHE**	**RSD%**	**SA**	**RSD%**	**MHE**	**RSD%**
1	2,3-pentanedione	111	17.97	152	5.14	2379	4.08	2487	20.93	27	20.17	92	11.23	513	0.86	628	1.22
2	hexanal	246	4.89	256	0.81	1343	*52.00*	54	2.07	444	14.2	1400	6.76	736	*45.16*	601	*50.48*
3	1-methyl-1(H)-pyrrole	278	7.38	305	5.72	1370	4.70	1283	18.30	82	15.68	258	13.59	1030	10.38	1072	4.54
4	heptanal	32	5.05	15	2.11	29	20.69	21	6.97	47	20.41	52	4.78	560	12.11	168	6.06
5	pyridine	168	17.79	239	2.07	663	13.28	730	2.51	113	1.5	215	0.85	375	6.52	409	2.84
6	2-methylpyrazine	318	11.54	429	5.47	1884	0.58	1926	4.03	129	7.87	216	8.36	736	3.08	810	4.35
7	3-hydrox-2-butanone	399	16.15	447	1.14	1565	*41.98*	1838	6.57	117	25.7	306	4.28	390	10.04	478	14.8
8	5-methyl-(*E*)-2-hepten-4-one	987	6.38	898	10.32	1267	4.21	1299	0.65	336	9.93	403	4.66	525	17.41	441	23.29
9	octanal	92	23.17	167	3.23	132	0.88	183	3.23	192	14.01	238	4.16	750	7.89	408	10.95
10	nonanal	603	*74.70*	87	6.26	594	*41.00*	105	9.43	920	*90.8*	198	2.06	3407	*48.00*	327	4.08
11	(*E*)-2-octenal	< LOQ	-	< LOQ	-	< LOQ	-	< LOQ	-	108	14.15	214	12.87	166	11.97	190	1.3
12	3-ethyl-2,5-dimethylpyrazine	342	7.37	209	5.35	1127	5.94	1386	5.22	95	7.62	110	13.81	364	3.34	468	2.85
13	furfural	251	22.24	331	3.17	5461	0.49	9393	7.09	310	7.18	365	11	4744	0.49	4178	0.7
14	2-ethyl-3,5-dimethylpyrazine	97	8.16	55	23.33	245	13.70	342	11.13	23	11.99	10	*36.7*	290	13.14	375	4.11
15	phenylacetaldehyde	41	12.86	251	1.38	1219	7.77	1383	12.07	32	10.18	249	-	267	18.23	362	21.03
16	(*E*)-2-decenal	< LOQ	-	< LOQ	-	< LOQ	-	< LOQ	-	< LOQ		< LOQ	-	351	7.89	244	4.96
17	3-methylbutanoic acid	191	4.50	238	7.64	85	19.87	290	8.48	34	12.11	202	2.04	230	25.40	202	0.77
18	2-phenylethanol	107	2.66	77	1.36	91	16.89	82	6.54	127	21.61	82	2.73	90	17.78	77	0.47
19	acetylpyrrole	273	2.92	181	9.03	448	6.09	647	13.75	227	2.42	176	2.17	519	8.06	396	3.78

Table 5

		Sample #1		Sample #2		Sample #3		Sample #4		Sample #5	
ID	**Compound name**	**(ng/g)**	**+/-**	**(ng/g)**	**+/-**	**(ng/g)**	**+/-**	**(ng/g)**	**+/-**	**(ng/g)**	**+/-**
1	2,3-pentanedione	< LOQ	-	< LOQ	-	< LOQ	-	< LOQ	-	< LOQ	-
2	hexanal	79	12	46	7	65	10	119	18	91	14
3	1-methyl-1(H)-pyrrole	< LOQ	-	< LOQ	-	< LOQ	-	< LOQ	-	< LOQ	-
4	heptanal	25	1	169	8	8	0	42	2	0	0
5	pyridine	206	4	192	4	189	4	188	4	189	4
6	2-methylpyrazine	106	6	88	5	99	5	101	6	106	6
7	3-hydrox-2-butanone	257	17	187	13	242	16	210	14	285	19
8	5-methyl-(*E*)-2-hepten-4-one	73	7	42	4	42	4	49	5	53	5
9	octanal	144	8	124	7	132	7	136	7	164	9
10	nonanal	94	5	3	0	12	1	11	1	0	0
11	(*E*)-2-octenal	< LOQ	-	< LOQ	-	< LOQ	-	< LOQ	-	< LOQ	-
12	3-ethyl-2,5-dimethylpyrazine	< LOQ	-	< LOQ	-	< LOQ	-	< LOQ	-	< LOQ	-
13	furfural	98	5	79	4	75	4	79	4	79	4
14	2-ethyl-3,5-dimethylpyrazine	4	1	3	0	1	0	2	0	7	1
15	phenylacetaldehyde	< LOQ	-	< LOQ	-	< LOQ	-	< LOQ	-	< LOQ	-
16	(*E*)-2-decenal	< LOQ	-	< LOQ	-	< LOQ	-	< LOQ	-	< LOQ	-
17	3-methylbutanoic acid	537	30	465	26	422	24	474	27	373	21
18	2-phenylethanol	163	5	72	2	77	2	81	2	74	2
19	acetylpyrrole	100	7	85	6	85	6	87	6	86	6

Figure 1: accuracy assessment results. Regression analysis on estimated concentrations for target analytes [ng/g] in TGT 170-35 and Ordu 170-35 samples. Outliers (linear and unsaturated aldehydes and furfural) are excluded.

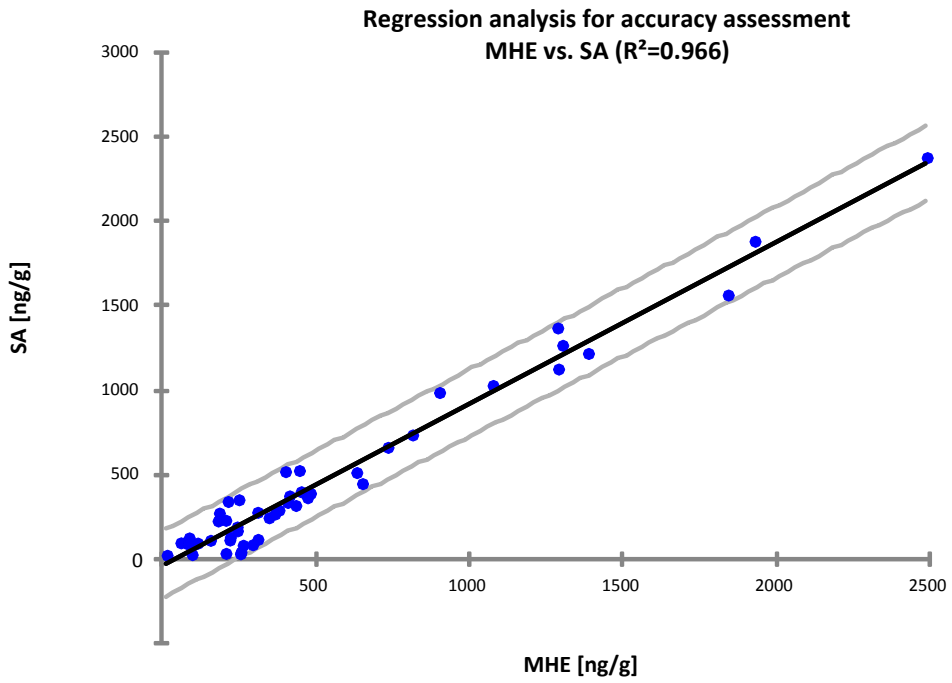

Figure 2: MHE slopes (β) for selected target analytes (5-methyl-*(E)*-2-hepten-4-one, 2-ethyl-3,5-dimethylpyrazine and 2-phenylethanol). The graphs are based on equal terms of cumulative response (A_T) arbitrarily fixed at 100 counts. Red and black lines show the logarithmic decay from calibration solutions in DBP-red and in cyclohexane-black (corresponding to calibrants in the gas phase approach) whereas blue and green lines indicate analyte behavior in hazelnuts and in the Gianduja paste, respectively.

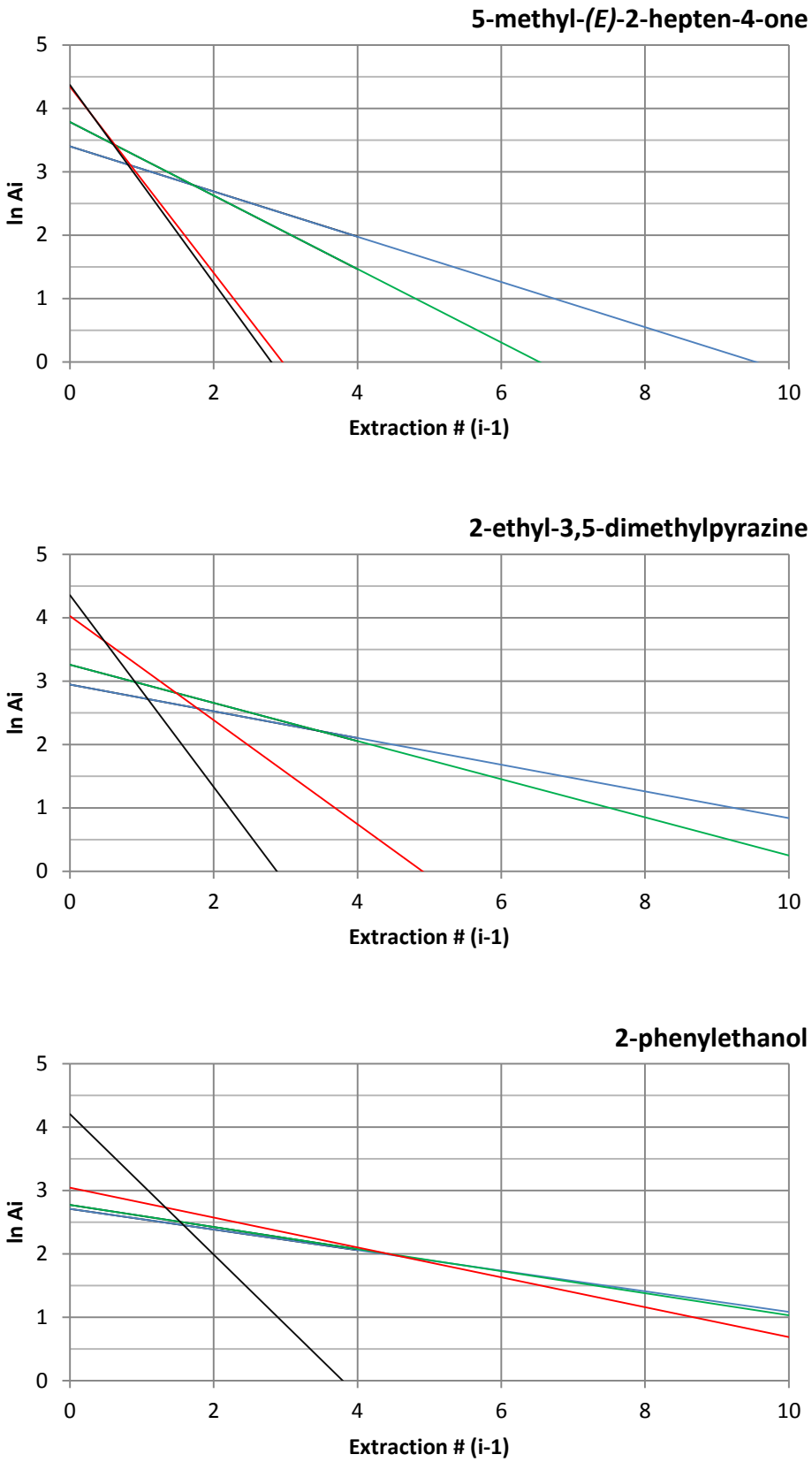

Figure 3: HS-SPME-GC×GC-MS patterns from different aliquots of TGT 170-35 together with fingerprinting results: Number of template peaks present in the *consensus template* (see text for details), Number reliably matched peaks, % of matching and identity of unmatched target peaks. Key-odorants are underlined.

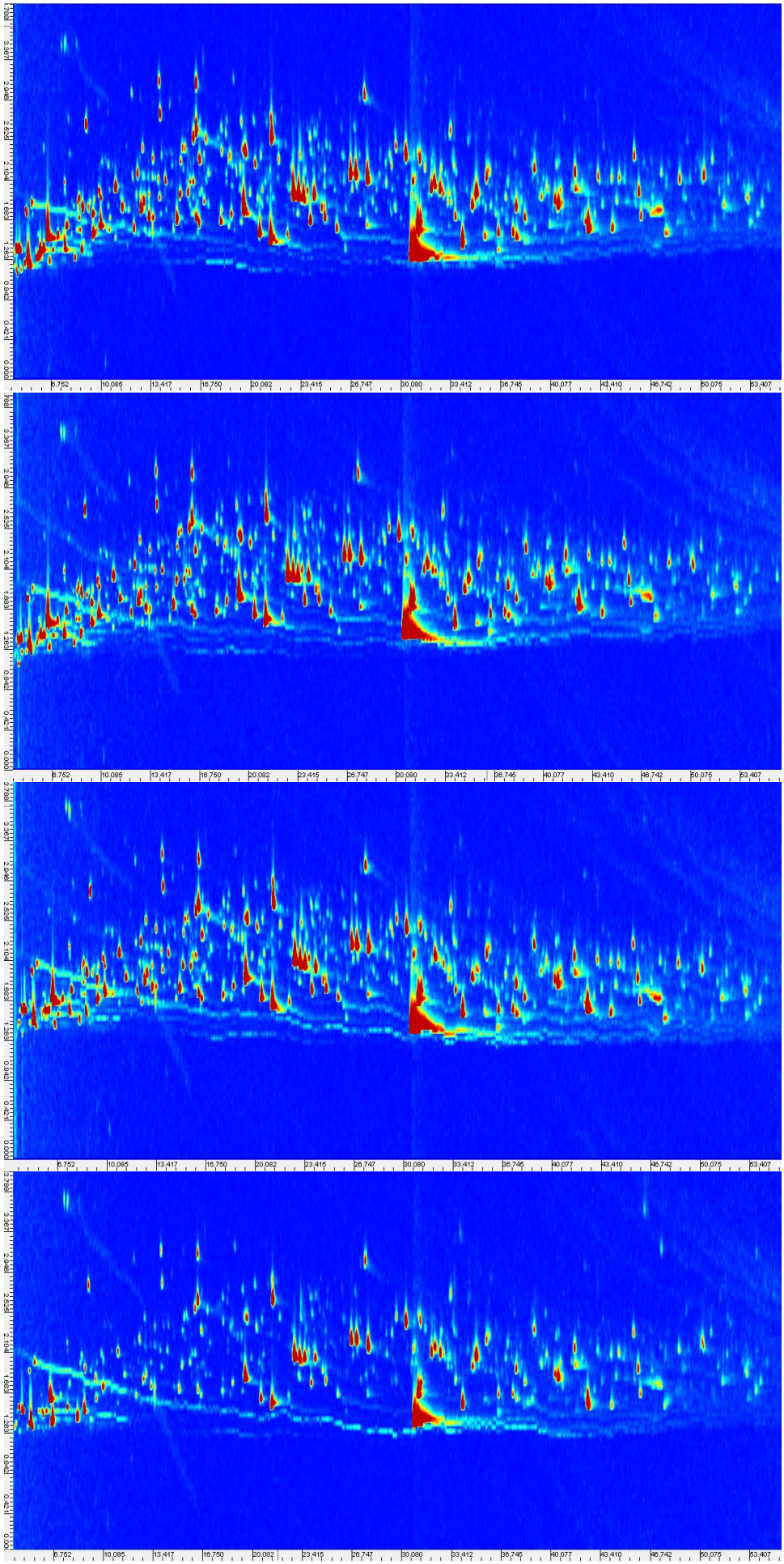

Sampling weight: 1.500 g
Template peaks: 355
Matched peaks: 355
% of Matching: 100%
Unmatched: -

Sampling weight: 1.000 g
Template peaks: 355
Matched peaks: 309
% of Matching: 92%
Unmatched peaks: 26

Unmatched Target peaks: 4
3-penten-2-one, 5-methyl-3-hepten-2-one, decanal, sabinene

Sampling weight: 0.500 g
Template peaks: 355
Matched peaks: 290
% of Matching 87%
Unmatched 45

Unmatched Target peaks: 8
1-cyclobutuylethanol, 2-ethyl-5-methylfuran, 2-methyl-2-pentenal, 3-penten-2-ol, 3-penten-2-one, 5-methyl-3-hepten-2-one, Decanal, sabinene

Sampling weight: 0.100 g
Template peaks: 355
Matched peaks: 245
% of Matching 73%
Unmatched 90

Unmatched Target peaks: 17
1-cyclobutuylethanol, 2-ethyl-5-methylfuran, 2-methyl-2-pentenal, 3-penten-2-ol, 3-penten-2-one, 5-methyl-3-hepten-2-one, decanal, sabinene, 2,4-dimethyl- 3-hexanone, 2-propylpiperidine, 3,3-dimethyl-1-butene, 4-methylpyridine, 3-methyl-3-butenoic acid, 2,3,5-trimethylfuran, 2-vinylfuran, 2-methylbutyl acetate, 2-acetyl-1-pyrroline

Figure 4: MHE slopes (β) for selected analytes not included in the pool of quantified targets.

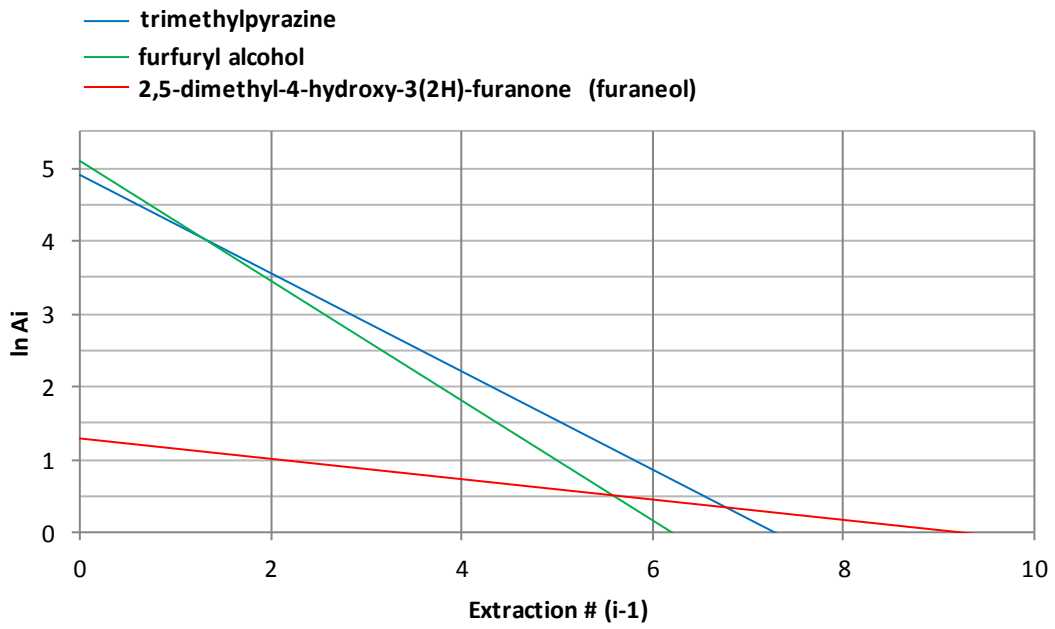

Tables

Table 1: List of target analytes considered in the quantitative fingerprinting, together with their CAS Registry Number, Purity % of the reference compound used for calibration, calculated physicochemical properties (Vapor Pressure – Vp and octanol/water partition coefficient – LogP), Target Ion and Qualifiers adopted for quantitation. Validation parameters include: calibration range, regression curves for SA and MHE calculated over six calibration points, coefficients of determination (R^2), Uncertainty % (Unc.%) and Limit of Determination (LOD) and Limit of Quantitation (LOQ). See text for details.

								Standard Addition			Multiple Headspace Extraction				
ID	**Compound name**	**CAS RN**	**Purity**	**Vp[a] (Torr, 25°C)**	**Log P[b]**	***Target Ion* Qualifiers**	**Range (ng/g)**	**Regression curve (n=6)**	**R^2**	**Unc.%**	**Regression curve (n=6)**	**R^2**	**Unc.%**	**LOD ng/g**	**LOQ ng/g**
1	2,3-pentanedione	600-14-6	97%	26.40	-0.831±0.297	*43*, 57, 100	10-2500	y = 3700.7x + 188647	0.991	10.8	y = 8015.6x + 37875	0.948	9.6	9.45	50.56
2	hexanal	66-25-1	98%	10.90	1.932±0.223	*44*, 56, 82	10-1500	y = 2642x + 297645	0.969	29.1	y = 5856.7x + 120348	0.999	15.0	2.60	11.48
3	1-methyl-1(H)-pyrrole	96-54-8	98%	25.60	1.351±0.251	*81*, 80, 53	10-1500	y = 567.92x + 39891	0.993	10.3	y = 1047.2x - 21952	0.974	10.5	12.19	51.89
4	heptanal	111-71-7	92%	3.85	2.442±0.223	*44*, 70, 55	10-1500	y = 967.76x + 58880	0.923	14.6	y = 2683.4x + 4197.7	0.999	5.0	1.12	5.64
5	pyridine	110-86-1	98%	22.80	0.836±0.178	*79*, 52, 51	10-1500	y = 821.45x + 49360	0.993	9.8	y = 2021x - 36590	0.979	2.1	10.58	50.34
6	2-methylpyrazine	109-08-0	99%	9.69	0.342±0.236	*94*, 67, 53	100-2500	y = 5582.8x + 989884	0.947	5.8	y = 14211x - 103899	0.997	5.6	5.02	22.36
7	3-hydrox-2-butanone	513-86-0	96%	1.92	-0.299±0.287	*45*, 43, 88	100-2500	y = 1772.9x + 195105	0.984	23.5	y = 16032x - 241081	0.955	6.7	2.22	11.21
8	5-methyl-(*E*)-2-hepten-4-one	102322-83-8	98%	1.25	2.023±0.252	*69*, 98, 111	100-2500	y = 10184x + 721440	0.997	9.5	y = 24400x - 62922	0.983	9.7	2.05	10.36
9	octanal	124-13-0	99%	2.07	2.951±0.223	*43*, 56, 84	10-1500	y = 1045.3x + 61668	0.993	11.5	y=2343.7x - 29123	0.978	5.4	6.24	27.58
10	nonanal	124-19-6	95%	0.53	3.461±0.223	*57*, 41, 70	10-4000	y = 1590.5x + 142268	0.981	63.6	y = 3339.4x + 5118.2	0.993	5.5	0.23	0.91
11	(*E*)-2-octenal	2548-87-0	94%	0.55	2.809±0.282	*41*, 55, 70	100-2500	y = 1582.3x + 23986	0.995	13.1	y = 6291.8x - 91734	0.953	7.1	11.45	49.46
12	3-ethyl-2,5-dimethylpyrazine	13360-65-1	98%	1.21	1.457±0.318	*135*, 136, 108	10-1500	y = 622.15x + 67165	0.966	6.1	y = 3596.5x + 68708	0.999	4.5	0.38	1.50
13	furfural	98-01-1	99%	2.23	0.712±0.264	*96*, 95, 39	100-10000[c]	y = 5694.8x + 3E+06	0.998	7.6	y = 12439x - 72625	0.989	5.5	6.10	24.46
14	2-ethyl-3,5-dimethylpyrazine	13925-07-0	98%	0.81	1.457±0.318	*135*, 136, 108	10-1500	y = 1225.6x + 25489	0.941	11.7	y = 4537x + 1419.7	0.974	18.8	0.37	0.90
15	phenylacetaldehyde	122-78-1	95%	0.37	1.760±0.224	*91*, 120, 65	10-1500	y = 3996.1x + 75391	0.986	12.3	y = 15521x - 362929	0.987	11.5	5.73	25.55
16	(*E*)-2-decenal	3913-81-3	92%	0.07	3.828±0.282	*41*, 55, 70	10-1500	y = 77.653x + 2728	0.941	7.9	y = 3324.4x - 68279	0.975	5.0	4.70	23.57
17	3-methylbutanoic acid	503-74-2	99%	0.55	1.051±0.193	*60*, 74, 87	10-1500	y = 2653x + 50140	0.991	15.5	y = 12958x - 242712	0.959	5.6	1.75	5.28
18	2-phenylethanol	60-12-8	98%	0.07	1.504±0.186	*91*, 122, 65	10-1500	y = 1886.7x + 14875	0.971	14.7	y = 20548x - 136118	0.971	2.8	5.47	24.36
19	acetylpyrrole	1072-83-9	99%	0.11	0.911±0.312	*94*, 109, 66	10-1500	y = 1188.7x + 55489	0.957	4.9	y = 11349x - 166508	0.974	7.2	1.59	5.35

[a,b]: Calculated using Advanced Chemistry Development (ACD/Labs) Software V11.02 (© 1994-2013 ACD/Labs)(Toronto, ON, Canada)

[c]: calibration was performed in two intervals (100-2500 and 2500-10000)– MHE and SA calibration curves reported are referred to 100-2500 ng/g

Table 2: Multiple Headspace Extraction calibration parameters. β values and coefficient of determination (R^2) for target analytes in hazelnut samples differing for geographical origin (Tonda Gentile Trilobata TGT and Ordu) and roasting conditions. Last two columns report calibration slopes in different media Dibutyl Phtalate DBP and Cyclohexane (equivalent to Gas Phase).

		TGT 170-20		TGT 170-35		Ordu 170-20		Ordu 170-35		Summary		Calibration slopes	
ID	**Compound name**	**β**	**R^2**	**β**	**R^2**	**β**	**R^2**	**β**	**R^2**	**β av**	**RSD%**	**β_{DBP}**	**β_{GP}**
1	2,3-pentanedione	0.67	0.979	0.76	0.995	0.61	0.935	0.66	0.979	0.62	9.00	0.42	0.39
2	hexanal	0.70	0.998	0.71	0.929	0.54	0.987	0.65	0.964	0.66	8.69	0.31	0.32
3	1-methyl-1(H)-pyrrole	0.63	0.981	0.77	0.971	0.55	0.909	0.60	0.889	0.57	12.44	0.19	0.13
4	heptanal	0.58	0.884	0.56	0.997	0.57	0.962	0.65	0.989	0.60	6.13	0.19	0.18
5	pyridine	0.45	0.989	0.50	0.959	0.39	0.908	0.51	0.973	0.48	12.72	0.48	0.50
6	2-methylpyrazine	0.62	0.901	0.63	0.982	0.52	0.979	0.62	0.995	0.60	9.32	0.21	0.19
7	3-hydrox-2-butanone	0.70	0.945	0.87	0.929	0.72	0.950	0.89	0.967	0.79	9.93	0.65	0.75
8	5-methyl-(*E*)-2-hepten-4-one	0.64	0.994	0.76	0.969	0.69	0.987	0.70	0.997	0.70	6.39	0.23	0.21
9	octanal	0.77	0.926	0.66	0.906	0.67	0.927	0.80	0.992	0.70	8.54	0.15	0.12
10	nonanal	0.81	0.904	0.85	0.929	0.82	0.925	0.63	0.767	0.80	10.36	0.48	0.31
11	(*E*)-2-octenal	< LOD	-	< LOD	-	0.95	0.988	0.83	0.914	0.84	14.46	0.41	0.26
12	3-ethyl-2,5-dimethylpyrazine	0.86	0.993	0.87	0.983	0.60	0.963	0.92	0.903	0.82	14.18	0.40	0.19
13	furfural	0.61	0.975	0.70	0.985	0.66	0.976	0.74	0.995	0.68	8.45	0.11	0.09
14	2-ethyl-3,5-dimethylpyrazine	0.74	0.936	0.88	0.948	0.76	0.969	0.90	0.948	0.81	11.05	0.44	0.22
15	phenylacetaldehyde	0.90	0.932	0.80	0.998	0.79	0.992	0.79	0.967	0.83	5.52	0.49	0.23
16	(*E*)-2-decenal	< LOD	-	< LOD	-	0.79	0.992	0.79	0.954	0.82	5.72	0.76	0.26
17	3-methylbutanoic acid	0.90	0.982	0.85	0.904	0.66	0.987	0.85	0.974	0.82	9.27	0.57	0.81
18	2-phenylethanol	0.90	0.932	0.89	0.957	0.89	0.998	0.88	0.980	0.85	6.71	0.79	0.33
19	acetylpyrrole	0.86	0.990	0.92	0.993	0.88	0.992	0.95	0.899	0.89	7.21	0.77	0.31

Table 3: Multiple Headspace Extraction calibration parameters. β values and coefficients of determination (R^2) for target analytes in *Gianduja* samples differing in formulation and manufacturer (Samples # 1-4 and Sample #5, respectively). The two right-hand columns report average values and precision (Relative Standard Deviation %).

		Sample #1		**Sample #2**		**Sample #3**		**Sample #4**		**Sample #5**			
ID	**Compound name**	**β**	**R^2**	**β**	**R^2**	**β**	**R^2**	**β**	**R^2**	**β**	**R^2**	**β av**	**RSD%**
1	2,3-pentanedione	< LOQ	-	< LOQ	-	< LOQ	-	< LOQ	-	< LOQ	-	-	-
2	hexanal	0.81	0.988	0.77	0.982	0.79	0.966	0.85	0.954	0.83	0.996	0.81	3.88
3	1-methyl-1(H)-pyrrole	< LOQ	-	< LOQ	-	< LOQ	-	< LOQ	-	< LOQ	-	-	-
4	heptanal	0.58	0.985	0.38	0.848	0.49	0.971	0.44	0.958	0.60	0.879	0.54	12.65
5	pyridine	0.59	0.994	0.28	0.822	0.28	0.822	0.48	0.985	0.48	0.989	0.42	12.26
6	2-methylpyrazine	0.66	0.961	0.56	0.974	0.80	0.982	0.74	0.978	0.52	0.933	0.66	12.63
7	3-hydrox-2-butanone	0.86	0.976	0.65	0.992	0.90	0.925	0.82	0.963	0.62	0.956	0.81	9.19
8	5-methyl-(*E*)-2-hepten-4-one	0.59	0.999	0.51	0.962	0.51	0.985	0.58	0.984	0.63	0.967	0.56	9.06
9	octanal	0.53	0.851	0.53	0.851	0.60	0.979	0.69	0.984	0.81	0.974	0.61	13.85
10	nonanal	0.76	0.809	0.32	0.940	0.77	0.859	0.78	0.962	0.78	0.962	0.76	3.29
11	(*E*)-2-octenal	< LOQ	-	< LOQ	-	< LOQ	-	< LOQ	-	< LOQ	-	-	-
12	3-ethyl-2,5-dimethylpyrazine	0.60	0.910	0.60	0.944	0.66	0.886	0.72	0.993	0.86	0.953	0.67	10.57
13	furfural	0.71	0.953	0.57	0.930	0.58	0.945	0.53	0.996	0.53	0.978	0.58	12.35
14	2-ethyl-3,5-dimethylpyrazine	0.54	0.928	0.78	0.989	0.72	0.999	0.72	0.993	0.83	0.929	0.74	9.69
15	phenylacetaldehyde	< LOQ	-	< LOQ	-	< LOQ	-	< LOQ	-	< LOQ	-	-	-
16	(*E*)-2-decenal	< LOQ	-	< LOQ	-	< LOQ	-	< LOQ	-	< LOQ	-	-	-
17	3-methylbutanoic acid	0.81	0.981	0.49	0.930	0.63	0.982	0.69	0.978	0.69	0.994	0.66	7.75
18	2-phenylethanol	0.92	0.966	0.49	0.844	0.87	0.998	0.88	0.993	0.75	0.962	0.84	8.25
19	acetylpyrrole	0.84	0.976	0.74	0.935	0.78	0.990	0.84	0.982	0.70	0.985	0.78	7.82

Table 4: Quantitation results in hazelnut samples for accuracy assessment. Concentration is expressed in ng/g in the matrix, precision data is referred to replicate determination over three months (see text for validation details).

		TGT 170-20 conc (ng/g)				TGT 170-35 conc (ng/g)				ORDU 170-20 conc (ng/g)				ORDU 170-35 conc (ng/g)			
ID	**Compound name**	**SA**	**RSD%**	**MHE**	**RSD%**	**SA**	**RSD%**	**MHE**	**RSD%**	**SA**	**RSD%**	**MHE**	**RSD%**	**SA**	**RSD%**	**MHE**	**RSD%**
1	2,3-pentanedione	111	17.97	152	5.14	2379	4.08	2487	20.93	27	20.17	92	11.23	513	0.86	628	1.22
2	hexanal	246	4.89	256	0.81	1343	*52.00*	54	2.07	444	14.2	1400	6.76	736	*45.16*	601	*50.48*
3	1-methyl-1(H)-pyrrole	278	7.38	305	5.72	1370	4.70	1283	18.30	82	15.68	258	13.59	1030	10.38	1072	4.54
4	heptanal	32	5.05	15	2.11	29	20.69	21	6.97	47	20.41	52	4.78	560	12.11	168	6.06
5	pyridine	168	17.79	239	2.07	663	13.28	730	2.51	113	1.5	215	0.85	375	6.52	409	2.84
6	2-methylpyrazine	318	11.54	429	5.47	1884	0.58	1926	4.03	129	7.87	216	8.36	736	3.08	810	4.35
7	3-hydrox-2-butanone	399	16.15	447	1.14	1565	*41.98*	1838	6.57	117	25.7	306	4.28	390	10.04	478	14.8
8	5-methyl-(*E*)-2-hepten-4-one	987	6.38	898	10.32	1267	4.21	1299	0.65	336	9.93	403	4.66	525	17.41	441	23.29
9	octanal	92	23.17	167	3.23	132	0.88	183	3.23	192	14.01	238	4.16	750	7.89	408	10.95
10	nonanal	603	*74.70*	87	6.26	594	*41.00*	105	9.43	920	*90.8*	198	2.06	3407	*48.00*	327	4.08
11	(*E*)-2-octenal	< LOQ	-	< LOQ	-	< LOQ	-	< LOQ	-	108	14.15	214	12.87	166	11.97	190	1.3
12	3-ethyl-2,5-dimethylpyrazine	342	7.37	209	5.35	1127	5.94	1386	5.22	95	7.62	110	13.81	364	3.34	468	2.85
13	furfural	251	22.24	331	3.17	5461	0.49	9393	7.09	310	7.18	365	11	4744	0.49	4178	0.7
14	2-ethyl-3,5-dimethylpyrazine	97	8.16	55	23.33	245	13.70	342	11.13	23	11.99	10	*36.7*	290	13.14	375	4.11
15	phenylacetaldehyde	41	12.86	251	1.38	1219	7.77	1383	12.07	32	10.18	249	-	267	18.23	362	21.03
16	(*E*)-2-decenal	< LOQ	-	< LOQ	-	< LOQ	-	< LOQ	-	< LOQ		< LOQ	-	351	7.89	244	4.96
17	3-methylbutanoic acid	191	4.50	238	7.64	85	19.87	290	8.48	34	12.11	202	2.04	230	25.40	202	0.77
18	2-phenylethanol	107	2.66	77	1.36	91	16.89	82	6.54	127	21.61	82	2.73	90	17.78	77	0.47
19	acetylpyrrole	273	2.92	181	9.03	448	6.09	647	13.75	227	2.42	176	2.17	519	8.06	396	3.78

Table 5: Quantitation results in *Gianduja* paste. Concentration and corresponding uncertainty are expressed in ng/g in the matrix (see text for details)

		Sample #1		Sample #2		Sample #3		Sample #4		Sample #5	
ID	**Compound name**	**(ng/g)**	**+/-**	**(ng/g)**	**+/-**	**(ng/g)**	**+/-**	**(ng/g)**	**+/-**	**(ng/g)**	**+/-**
1	2,3-pentanedione	< LOQ	-	< LOQ	-	< LOQ	-	< LOQ	-	< LOQ	-
2	hexanal	79	12	46	7	65	10	119	18	91	14
3	1-methyl-1(H)-pyrrole	< LOQ	-	< LOQ	-	< LOQ	-	< LOQ	-	< LOQ	-
4	heptanal	25	1	169	8	8	0	42	2	0	0
5	pyridine	206	4	192	4	189	4	188	4	189	4
6	2-methylpyrazine	106	6	88	5	99	5	101	6	106	6
7	3-hydrox-2-butanone	257	17	187	13	242	16	210	14	285	19
8	5-methyl-(*E*)-2-hepten-4-one	73	7	42	4	42	4	49	5	53	5
9	octanal	144	8	124	7	132	7	136	7	164	9
10	nonanal	94	5	3	0	12	1	11	1	0	0
11	(*E*)-2-octenal	< LOQ	-	< LOQ	-	< LOQ	-	< LOQ	-	< LOQ	-
12	3-ethyl-2,5-dimethylpyrazine	< LOQ	-	< LOQ	-	< LOQ	-	< LOQ	-	< LOQ	-
13	furfural	98	5	79	4	75	4	79	4	79	4
14	2-ethyl-3,5-dimethylpyrazine	4	1	3	0	1	0	2	0	7	1
15	phenylacetaldehyde	< LOQ	-	< LOQ	-	< LOQ	-	< LOQ	-	< LOQ	-
16	(*E*)-2-decenal	< LOQ	-	< LOQ	-	< LOQ	-	< LOQ	-	< LOQ	-
17	3-methylbutanoic acid	537	30	465	26	422	24	474	27	373	21
18	2-phenylethanol	163	5	72	2	77	2	81	2	74	2
19	acetylpyrrole	100	7	85	6	85	6	87	6	86	6

Figure 1

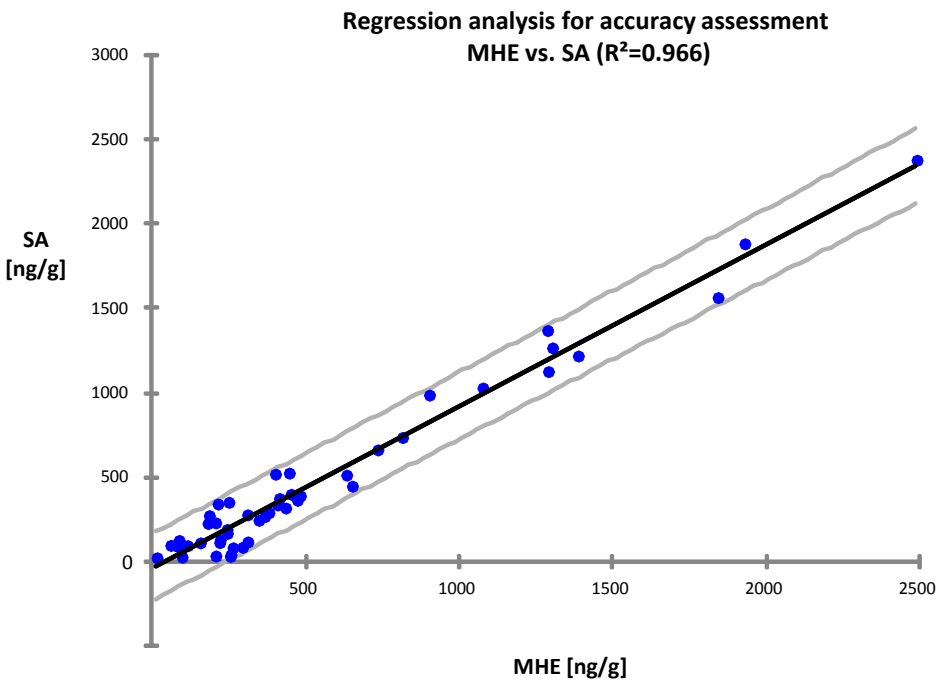
Regression analysis for accuracy assessment
MHE vs. SA (R^2=0.966)
SA
[ng/g]
3000
2500
2000
1500
1000
500
0
500
1000
1500
2000
2500
MHE [ng/g]

Figure 2

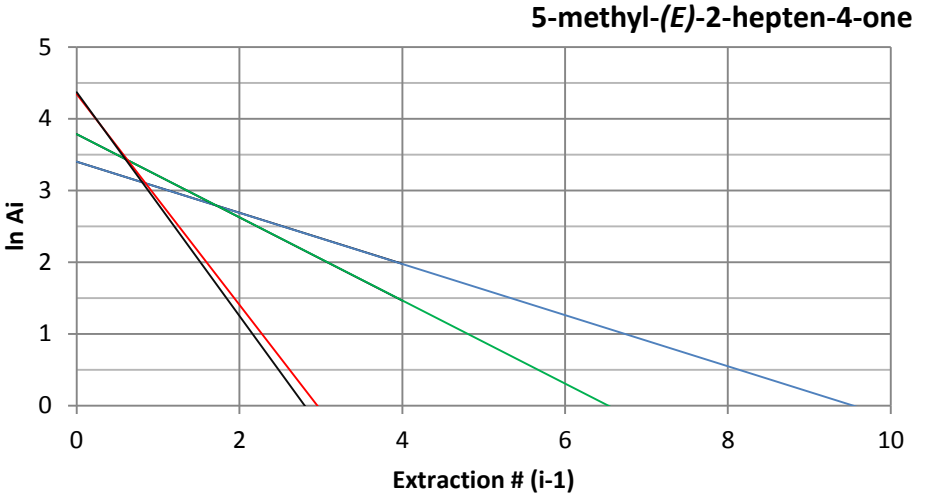
5-methyl-(E)-2-hepten-4-one
ln Ai
Extraction # (i-1)
0
1
2
3
4
5
0
2
4
6
8
10

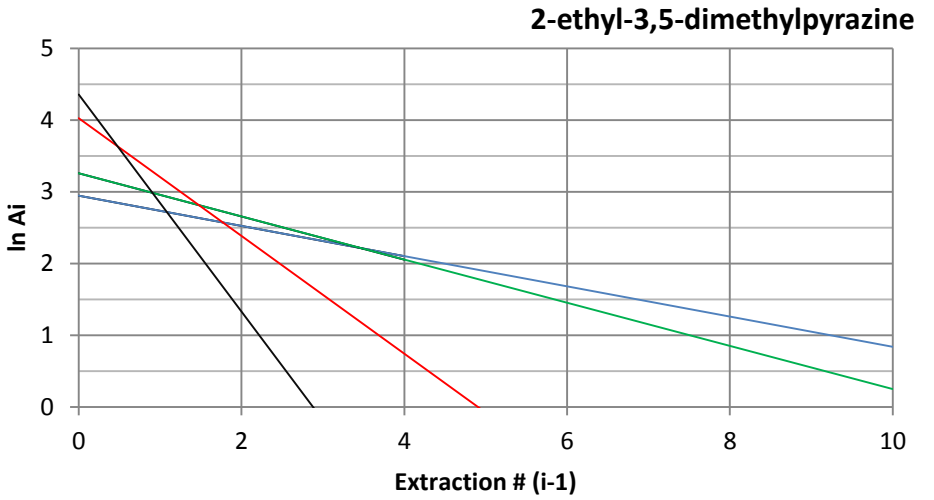
2-ethyl-3,5-dimethylpyrazine
ln Ai
Extraction # (i-1)
0
1
2
3
4
5
0
2
4
6
8
10

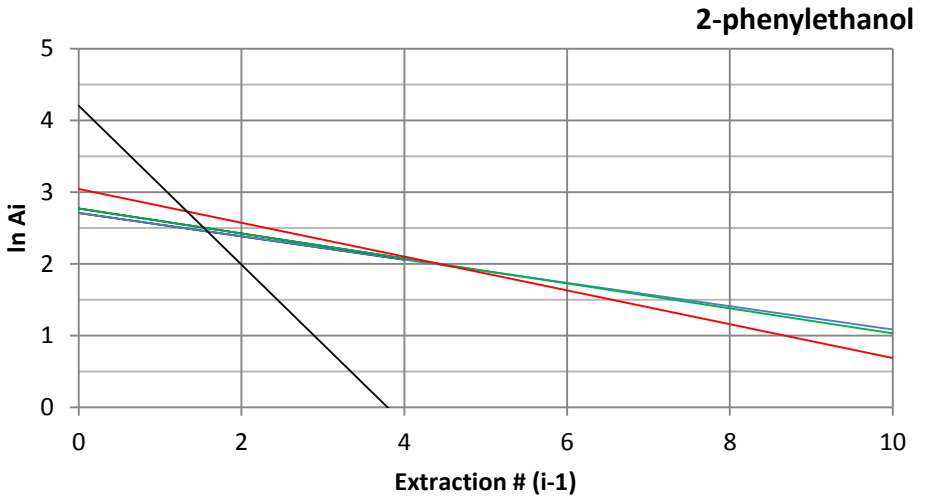
2-phenylethanol
ln Ai
Extraction # (i-1)
0
1
2
3
4
5
0
2
4
6
8
10

Figure 3

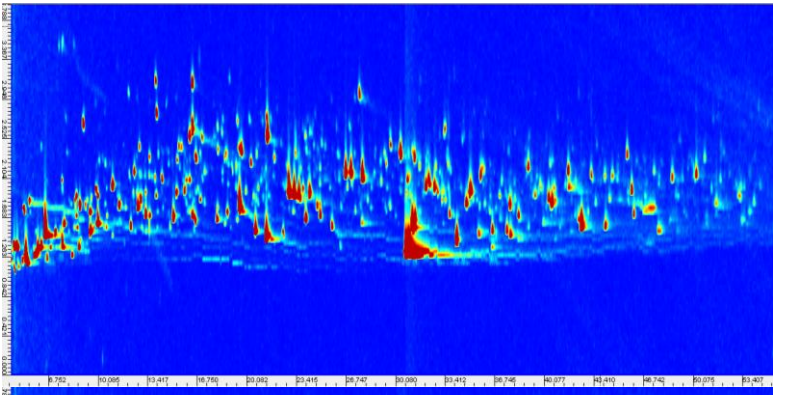

Sampling weight: 1.500 g
Template peaks: 355
Matched peaks: 355
% of Matching: 100%
Unmatched: -

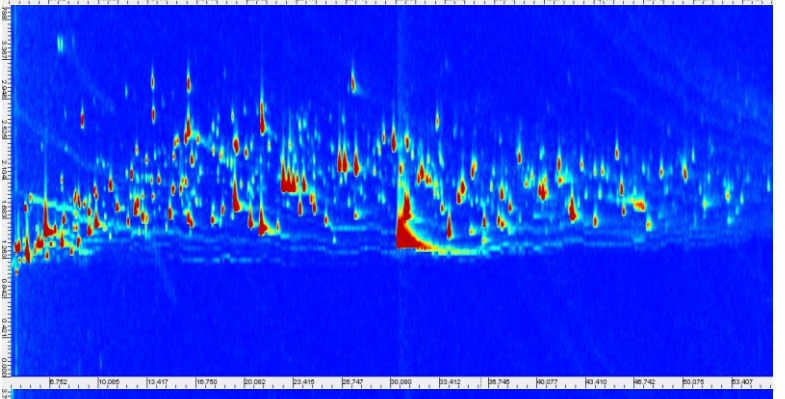

Sampling weight: 1.000 g
Template peaks: 355
Matched peaks: 309
% of Matching: 92%
Unmatched peaks: 26

Unmatched Target peaks: 4
3-penten-2-one, 5-methyl-3-hepten-2-one, decanal, sabinene

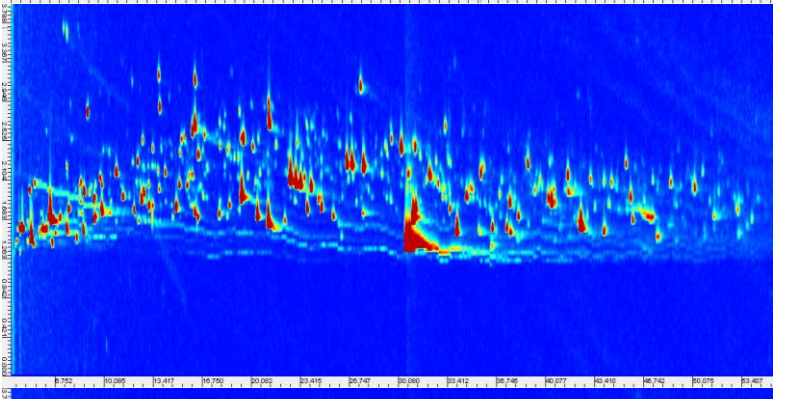

Sampling weight: 0.500 g
Template peaks: 355
Matched peaks: 290
% of Matching 87%
Unmatched 45

Unmatched Target peaks: 8
1-cyclobutuylethanol, 2-ethyl-5-methylfuran, 2-methyl-2-pentenal, 3-penten-2-ol, 3-penten-2-one, 5-methyl-3-hepten-2-one, Decanal, sabinene

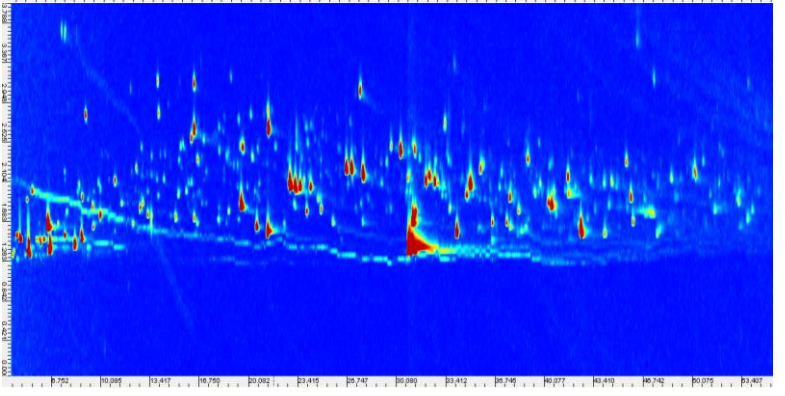

Sampling weight: 0.100 g
Template peaks: 355
Matched peaks: 245
% of Matching 73%
Unmatched 90

Unmatched Target peaks: 17
1-cyclobutuylethanol, 2-ethyl-5-methylfuran, 2-methyl-2-pentenal, 3-penten-2-ol, 3-penten-2-one, 5-methyl-3-hepten-2-one, decanal, sabinene, 2,4-dimethyl- 3-hexanone, 2-propylpiperidine, 3,3-dimethyl-1-butene, 4-methylpyridine, 3-methyl-3-butenoic acid, 2,3,5-trimethylfuran, 2-vinylfuran, 2-methylbutyl acetate, 2-acetyl-1-pyrroline

Figure 4

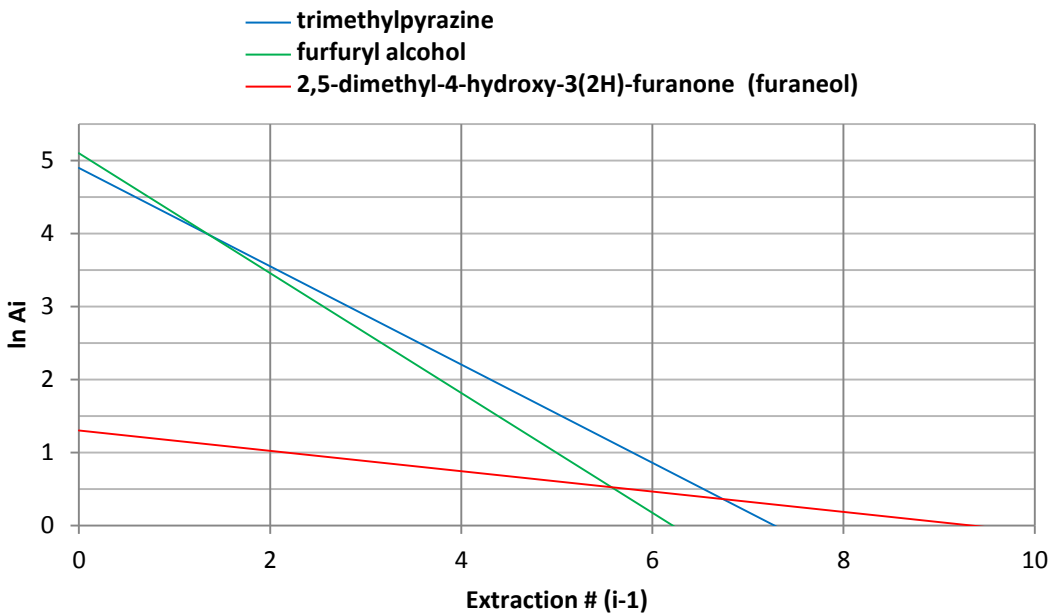
trimethylpyrazine
furfuryl alcohol
2,5-dimethyl-4-hydroxy-3(2H)-furanone (furaneol)
ln Ai
0
1
2
3
4
5
0
2
4
6
8
10
Extraction # (i-1)